PHOTODYNAMIC RELEASE OF NITRIC OXIDE FROM NITROSOTHIOLS OF GLUTATHIONE, AND SERUM ALBUMIN STUDIED BY TRANSIENT ABSORPTION AND TRANSIENT CIRCULAR DICHROISM SPECTROSCOPY

by

Rojana Leecharoen

B. A. in Chemistry, Washington University in St. Louis, 1996

Submitted to the Graduate Faculty of

Arts and Sciences in partial fulfillment

of the requirements for the degree of

M. S. in Physical Chemistry

University of Pittsburgh

2005

UNIVERSITY OF PITTSBURGH

ARTS AND SCIENCES

This thesis was presented

by

Rojana Leecharoen

It was defended on

February 4, 1999

and approved by

David N. Beratan, Professor of Chemistry

David H. Waldeck, Associate Professor of Chemistry

Thesis Advisor: Gilbert C. Walker, Assistant Professor of Chemistry

PHOTODYNAMIC RELEASE OF NITRIC OXIDE FROM NITROSOTHIOLS OF GLUTATHIONE, AND SERUM ALBUMIN STUDIED BY TRANSIENT ABSORPTION AND TRANSIENT CIRCULAR DICHROISM SPECTROSCOPY

Rojana Leecharoen, M. S.

University of Pittsburgh, 2005

Nitrosation of the free sulfhydryl group in peptides and proteins lead to one of their important biological functions; as nitric oxide carriers. Nitric oxide, an important signally free radical molecule cannot travel to many of its important targets by itself due to its short half-life. The S-NO bond in S-nitrosopeptides or proteins, however, is both thermolytically and photolytically labile, leading to release of NO which can then attack other targets such as other amino acids and nucleotides. In this thesis, photodynamic activity of NO released from a model peptide (glutathione) and a model protein (bovine serum albumin) is studied utilizing various spectroscopic tools. The more simple linear transient absorption spectroscopy gives information on the time-scale of the photocleavage as well as that of the subsequence geminate recombination, while the more difficult transient circular dichroism will give more insightful into the conformation changes of the peptide and protein surrounding the chromophore and the direction at which the NO is being released which will enable us to explore possible targets of the photoreleased NO. In addition to experimental study, many theoretical calculations are performed to aid understanding of the results.

TABLE OF CONTENTS

LIST OF TABLES

LIST OF FIGURES

1.0 OVERALL GOALS

- To characterize the set of equilib rium and reactive conform ations of NO bound to peptides or protein nitrosothiols using spectroscopy and computer simulation.
- To use time-resolved infrared absorbance and visible circular dichroism spectroscopy to measure the kinetics of photocleaved NO m igration and to identify the response of the protein and solvent.

2.0 INTRODUCTION

2.1 WHAT IS NITRIC OXIDE?

Nitric oxide is one simplest heteronuclear diatomic molecules known to chemists, yet it can perform many sophisticated functions in both physical and biological systems. During the past 50 years, it has become one of the molecules most studied. This small molecule can do both good and harm. In addition to being a common air pollutant, it can also safeguard life on Earth by playing an important role in the rate of the reduction of the ozone layer.[1,2] Much research addresses roles of nitric oxide in living bodies. Robert Furchgott, Louis Ignarro, and Ferid Murad who received the Nobel Prize for Physiology and Medicine in 1998, showed that the endothelium-derived relaxing factor is in fact nitric oxide and that the drug nitroglycerine reduces chest pain by releasing nitric oxide which affects the vascular smooth muscle.[3-5] The vasodiatory role of nitric oxide led to a recently discovered drug with the commercial name "Viagra" (sildenafil citrate). The drug works by releasing nitric oxide in the corpus cavernosum in response to sexual stimulation. NO activates the enzyme guanylate cyclase, which results in locally increased levels of cGMP, thereby producing smooth muscle relaxation. In addition to its signaling role in cardiovascular system, it also acts as a signal molecule in the nervous system[6,7], as a blood pressure regulator, and prevents the formation of thrombi. When it is produced in large quantity in white blood cells, it can become toxic to invading bacteria and parasites.[8,9] It can cause cell apoptosis which makes it a center of interest for many cancer researchers.[10,11]

2.2 HOW IS NO REGULATED IN LIVING BODIES?

In living bodies, nitric oxide is synthesized from the amino acid L-arginine by the enzyme nitric oxide syntase (NOS). NO reacts quickly with oxygen and superoxide and forms other oxides of nitrogen, some of which are toxic. However, *in vivo*, the lifetime of NO is lengthened and the concentration of the free NO is regulated through binding with several acceptors such as metals (an example is the binding of NO with the heam in heamoglobin) and thiols.[12] Figure 1 illustrates how NO is regulated in biological systems.

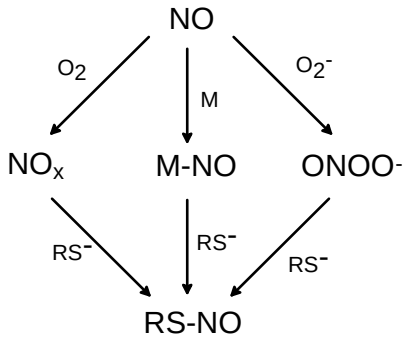

Figure 1: Schematic representation of biological NO regulation pathways.
Many roads lead to nitrosothiols

Recent studies have shown that nitrosothiols could be used therapeutically as NO-producing drugs in place of the glycerol trinitrate, which is commonly used to treat cardiac disease.[13] The most abundant of S-nitrosothiols among peptides and proteins are S-nitrosoglutathione (GS-NO) and S-nitrosoalbumin (SA-NO). NO binds to the sulfhydryl cysteine. Glutathione, because of its small size, is a main intercellular carrier of nitric oxide and consequently is regarded as a main scavenger of NO both inside and outside the cell, leading to its role as a detoxification agent. GS-NO has been measured at micromolar concentrations in human bronchial fluid and been shown to be vasodilatory.[14] However, its low stability and its low concentration in plasma prohibit it from being the main carrier of nitric oxide in the body. The protein species regarded as a

main carrie r of nitric oxide in most m ammals is the p lasma protein called se rum albumin.[15]

2.3 RELEVANCE OF PHOTODYNAMICS OF S-NITROSOTHIOL OF PEPTIDES AND PROTEINS

The S-NO bond breaks when the system is photoexcited from $S_0 \rightarrow S_1$ or $S_0 \rightarrow S_2$, which means that $NO^{\cdot}$ (or NO^+ if the bond cleaves heteroly tically) will be released.[16] Since the concentration of free NO is critical for any living body, identifying the fate of the photoreleased NO becom es a very interestin g subject for research. Even though the photolytic pathway cannot occur deep with in m ammalian bodies, our prelim inary calculation has shown that the rate of NO p hotocleavage in sk in capillaries d ue to sunlight (mM/hr) can exceed the rate due to th ermal pathways[17]. Moreover, there has been a suggestion that photoinduced processe s in NO m etabolism influence the circadian rhythm[18]. So far there have been no m echanistic studies of photoinduced NO-cleavage from the m ain carrier, SA-NO and no de tailed m easurements on nitrosopeptides, therefore this work will be the first study that tr ies to answer one f undamental question: "What are the paths and products of photoi nduced NO loss from SA-NO and GS-NO, and what are their biochemical implications?"

3.0 BACKGROUND AND THEORY

3.1 WHY DO THIOLS HOST NO?

Thiols are compounds that contain the S-H functional group. The cloud of electrons surrounding the nucleus of the sulfer atom is highly polarizable, making the sulfhydryl group a good nucleophile for reactions with electrophilic compounds such as NO. S-Nitrosothiols (RSNOs), sometimes called thionitrites, are the sulfur analogs of the alkyl nitrites RONO. They have come to prominence in NO biochemistry because they are believed to decompose nonenzymatically *in vivo* to yield NO. Nevertheless, how S-nitrosothiols are initially formed *in vivo* is still heavily debated. NO itself is a very unlikely direct nitrosating agent. Several groups [19,20] have studied the kinetics of nitrosation of thiols with oxygenated NO solution and have concluded that the most likely nitrosating agent is N_2O_3. Goldstein and co-workers [19], for example, argue that S-Nitrosothiol formation from free NO *in vivo* is unlikely. Others pathway maybe more likely such as transnitrosation.[21]

S-Nitrosothiols have not received extensive attention in chemistry because many of them are unstable at room temperature. Peptides and proteins, however, form stable nitrosothiols which range in color from green to red/orange; generally tertiary structures are green and primary ones (such as cysteine containing NOs) are red/orange. *In vitro*, nitrosothiols are readily formed from thiols and any electrophillic nitrosating agent[21], XNO, which acts as a reagent capable of delivering NO^+ as outlined in Equation 1.

$$RSH + XNO \longrightarrow RSNO + X^- + H^+ \quad (1)$$

The most commonly used reagent solution is an aqueous solution of nitrous acid generated from sodium nitrite and a mineral acid. Nitrosothiol formation from thiols is a very rapid process and when equimolar solutions of thiol and nitrite are mixed at room

temperature, the nitrosothiol is formed quantitatively within minutes. After adjustment of the solution pH, these solutions are sufficiently stable to allow experiments that require hours. It is equally possible to form nitrosothiols from thiols and alkylnitrites in aqueous acid or alkaline solutions or in some non-aqueous solvents such as acetone and chloroform.[22] The reaction mechanism, which is an electrophillic attack at the sulfur similar to the nitrosation of amines, alcohols and some aliphatic and aromatic systems, has been established for the nitrous acid reaction.[23] The reaction is catalyzed by acids and nucleophiles such as halides.

3.2 NO HOST BEING STUDIED

3.2.1 Cysteine

Cysteine is one of 20 known amino acids containing a thiol functional group as its side chain. The structure of S-nitrosocysteine (Cys-NO) is as shown in Figure 2

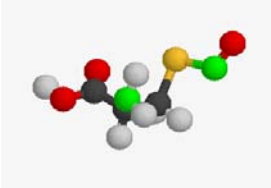

Figure 2: Chemical structure of Cys-NO

3.2.2 Glutathione

Glutathione (GSH) is a tripeptide g-L-glutamyl-L-cysteinylglycine (see Figure 3 for structure of S-nitrosoglutathione (GS-NO)). It is the most abundant cellular low-molecular-mass thiol; human erythrocytes contain 2 mM GSH and hepatocytes, greater than 10 mM. It is the sulfhydryl group of cysteine that plays a very important role in carrying NO[24].

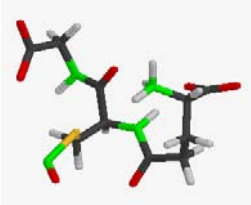

Figure 3: Chemical structure of GS-NO

3.2.3 Serum Albumin

Serum Albumin is a predominant protein in many mammalian bodies. It binds water, cations such as Ca^{2+}, Na^{+}, K^{+}, fatty acids, hormones, bilirubin and drugs. Despite the fact that its detailed structure varies from species to species, all known mammalian serum albumins have a similar pattern of intramolecular disulfide bonds (about 17 cystines) and contain one free cysteine at position 34. This cysteine does not participate in the intramolecular disulfide bonding so it is available for binding a ligand and forming intermolecular disulfide bonds. This free cysteine 34 and its dominance in blood plasma (60% total and about 42 g/L) cause serum albumin to be a main carrier of nitric oxide in most mammalian bodies *via* the nitrosothiol formation at the cysteine 34. In this study, only bovine serum albumin and human serum albumin proteins are to be studied. The two serum albumins are very similar. There is only one notable difference; HSA has only one tryptophan while BSA has two tryptophans. Many structural and chemical aspects of the two serum albumins (HSA and BSA) are well characterized. [25-27] BSA contains 580 amino acids per chain while HSA contains 585 amino acids. Figure 5 shows a comparison of the amino acid sequences of BSA and HSA. X-ray crystal structure

studies have shown that the tertiary structur e of HSA is heart-shaped o r an equilateral triangular molecule 80 Å on a side with average thickness of 30 Å. Cys-34 is found in the non-helical turn between helix 2 and helix 3 of domain IA. Severa l studies have shown that this free thiol lies in a sterically restricted e nvironment that has a hydrophobic character.[28] Figure 4 shows x-ray cr ystal structure of one ch ain of HSA in which the position of Cys-34 clearly indicated. The figur e also shows the position of tyrosine and tryptophan, both of whi ch are susceptible to nitrosylation though with the sm aller rate constant than Cys-34.[29]

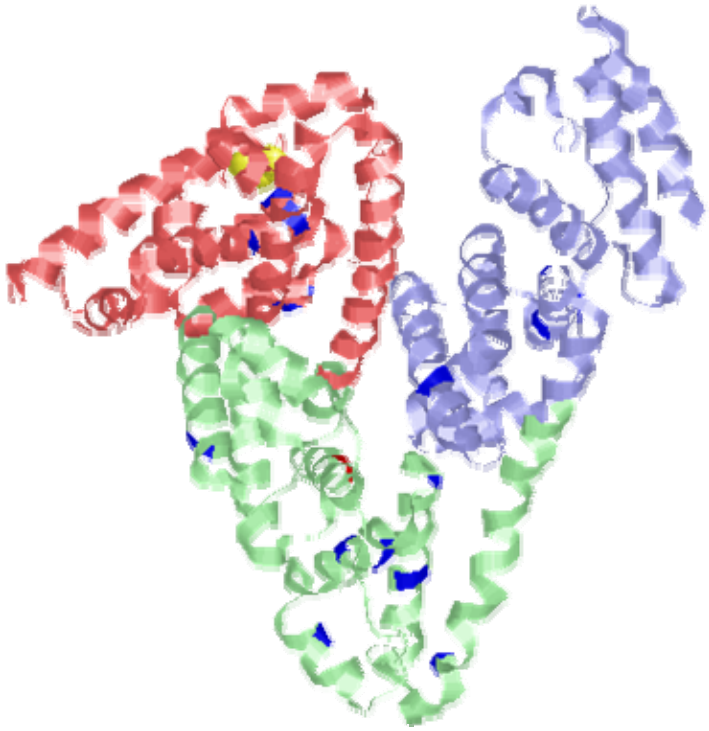

Figure 4: The heart-shaped HSA

The position of cysteine 34 is indicated by the yellow area. The blue spots correspond to positions of tyros ine an d red is f or tryptoph an. The chain is colo red accord ing to its domains. The light red is domain I, green is domain II and the purple is domain III.

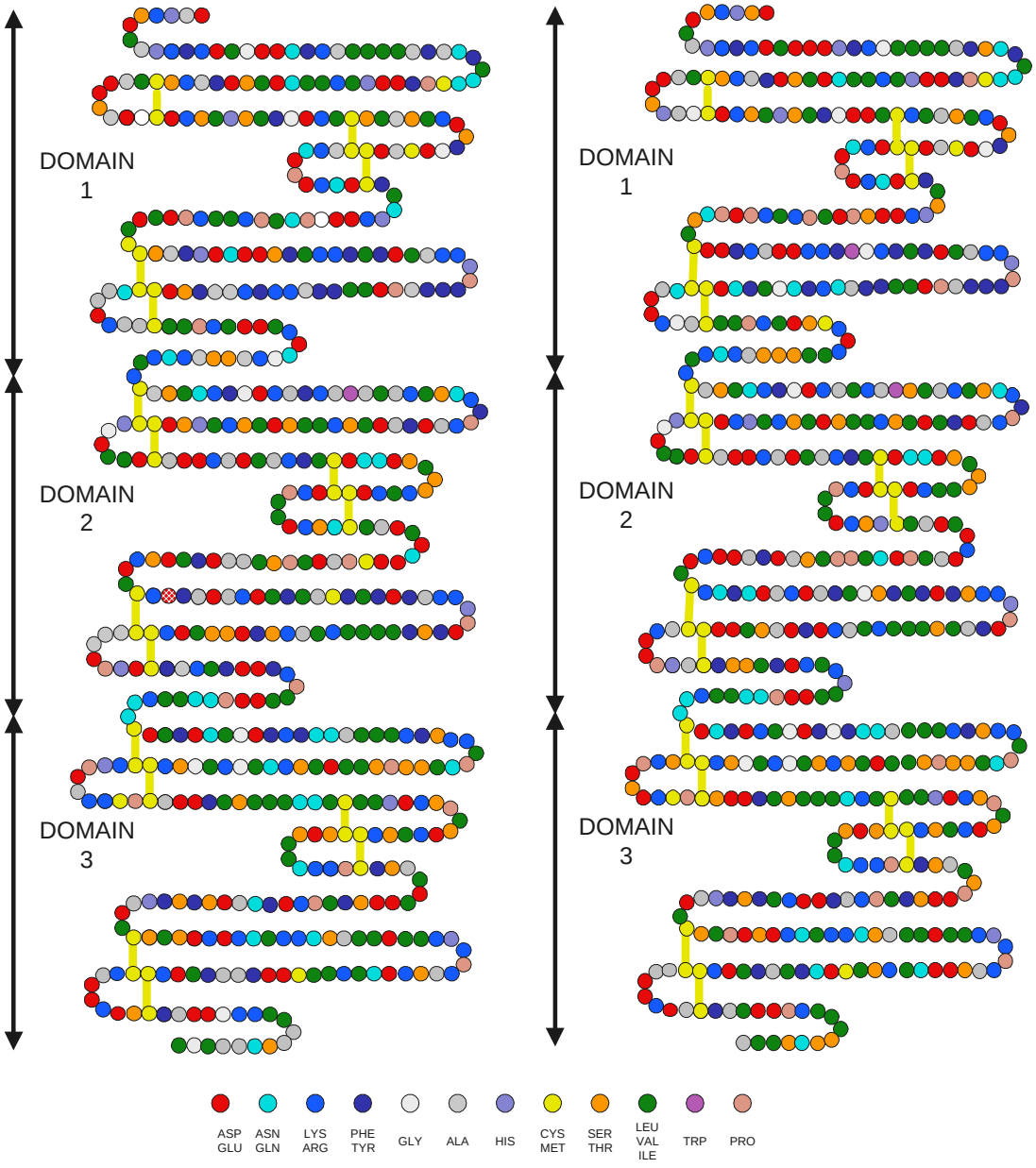

Figure 5: Human Serum Albumin (HSA), left and Bovine Serum Albumin (BSA), right

They are very sim ilar. The a mino acids are grouped based on their properties. The albumin chain is generally grouped into 3 domains. Each dom ain contains two long loops and one short loop.

3.3 ELECTRONIC PROPERTIES OF THE SYSTEMS

3.3.1 UV-visible spectra

The UV spectra of S-nitrosocysteine (Cys- NO), S-nitrosoglutathione (GS-NO) and S-nitroso bovine serum albumin (BSA-NO) as shown in Figure 6 reveal two bands centered at 550 nm and 335 nm, corresponding to $S_0 \rightarrow S_1$ and $S_0 \rightarrow S_2$ transitions respectively. The extinction coefficient of the 335 nm band is much higher than that of 550 nm band, which agrees well with m y theoretical calculations (see calcu lation section) indicating th at the 335 nm transition is electric dipole allowed whereas the 550 nm band is nearly forbidden. The extinction coefficient of BSA-NO at 335 nm is alm ost triple those of GS-NO and Cys-NO. The additional absorptivity m ight be partially due to a ni trosylated tryptophan chromophore, which reacts m ore slowly with nitrosating species (eith er N_2O_3 or NO_x) than Cys-34. N-nitrotrytophan also has an absorption band centered around 335 nm , and can be produced in acidic sodium nitrite solution.[29]

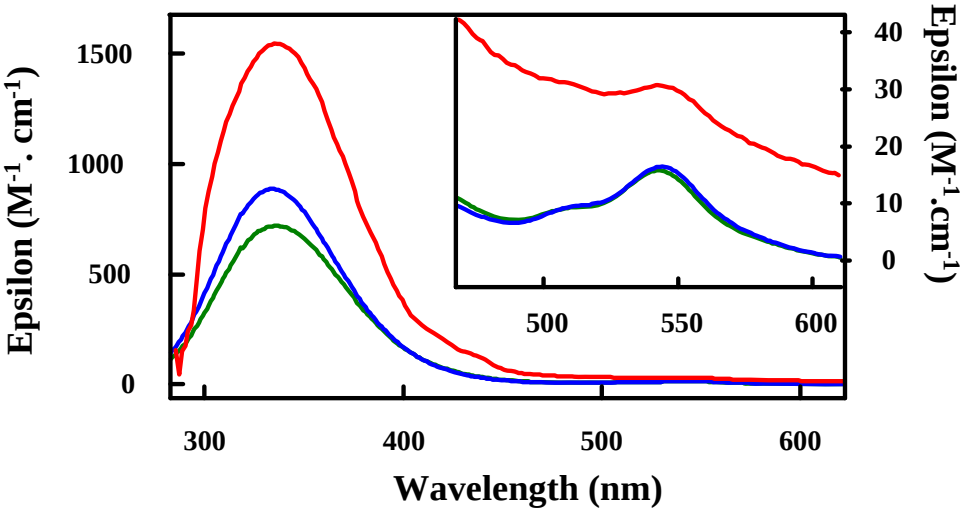

Figure 6: UV-Vis spectra
BSA-NO (red), GS-NO (blue) and Cys-NO (green)

3.3.1 Infrared spectra

Figure 7 shows the FTIR difference spectra of deuterated Cys-NO and GSNO. These spectra are plotted as the IR spectrum of RSNO minus the IR spectrum of RSH, with solvent and water vapor corrections. NO resonance frequencies and bandwidths depend on the peptide studied. In Cys-NO the NO band is found at *ca.* 1560 cm^{-1}, whereas it is found at *ca.* 1530 cm^{-1} in glutathione. These bands are quite wide in Cys-NO (78 cm^{-1}) and in GS-NO (67 cm^{-1}). They are too wide to result from a single characteristic chromophore. Rather, they probably result from the overlap of two or more species.

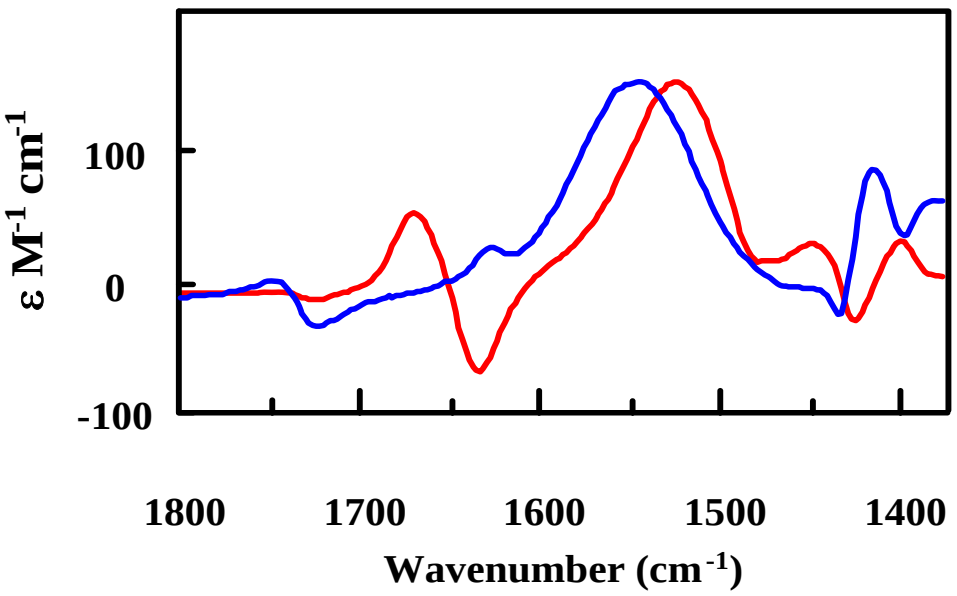

Figure 7: Infrared difference spectra

They reveal the characteristic feature of S-NO at ca. 1530 cm^{-1}. Other perturbations of the peptide backbone are described in the text. The Cys-NO (blue) and GS-NO (red) spectra are obtained as the IR spectrum of RSNO minus the IR spectrum of RSH, with solvent and vapor corrections.

The FTIR spectra show perturbations to the peptide backbone resonances in GS-NO, in the amide I' (~ 1650 cm^{-1}) and II' (~ 1450 cm^{-1}) regions. The amide I' band is frequency up-shifted by nitrosylation. The amide II' resonance is broadened. The integrated area of the amide I' response suggests that the effect corresponds to the displacement of *ca.* 20% of the oscillator strength. Interestingly, the change in the cysteine resonance is even smaller, suggesting that in GS-NO it is the non-cysteine carbonyls that are perturbed by nitrosylation of cysteine. The decreased quantum yield for dissociation of GS-NO over Cys-NO[30] is consistent with this observation, and suggests the larger peptide harbors the NO better.

Figure 8 shows the FTIR spectrum of deuterated BSA-NO. The assign peaks are COOH (1680-1710 cm^{-1}), Amide I' (1650 cm^{-1}), Amide II' (1450 cm^{-1}), COO^-_{ss} (1560-1400 cm^{-1}), Tyr (1517 cm^{-1}), side chain resonance (*ca.* 1450 cm^{-1}).

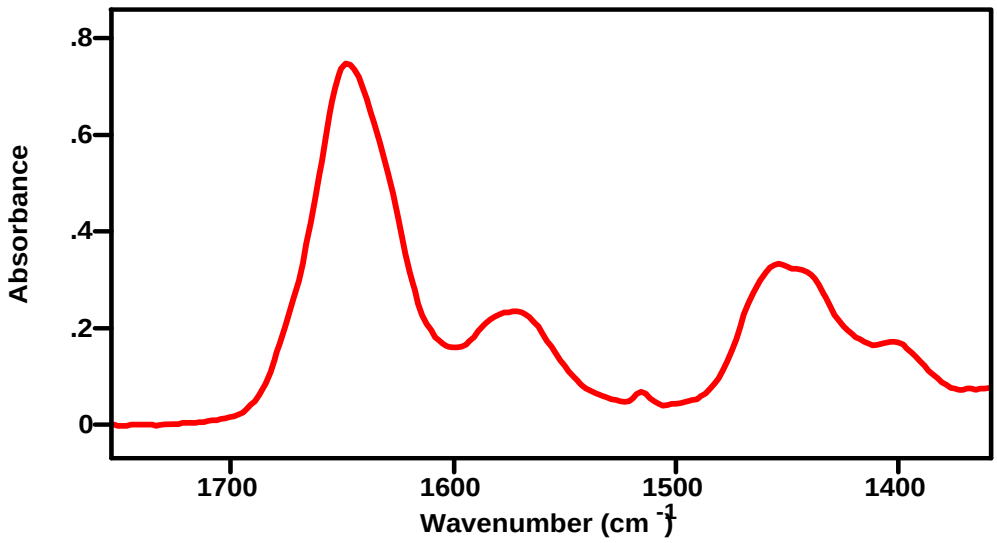

Figure 8: The infrared absorption spectrum

Sample is 755 μM deuterated BSA in D_2O (pH=7.20) after solvent subtraction.

3.3.3 Circular dichroism spectra

Circular dichroism (CD) is the difference in absorbance between left and right circularly polarized light. For peptides or proteins, it has been used as a tool to study protein conformation or peptide folding. Most of the CD measured in peptides or protein is due to conformation of the backbone since the transitions giving rise to the CD are usually n $\rightarrow \pi^*$ or $\pi \rightarrow \pi^*$ of the amide. This type of CD is typically broad, and usually appears at wavelengths below 300 nm. Fortunately for the S-nitrosothiol systems being studied, we found an isolated CD band of Cys-NO, GS-NO and BSA-NO center around 550 nm.[31] This band corresponds to the $S_0 \rightarrow S_1$ transition, which mainly involves the electron cloud around S-N bond rather than that around the backbone amide. Furthermore, for Cys-NO and GS-NO which do not have any CD signal due to the backbone in the region 300-400 nm, we see another distinct but rather weak CD band at 335 nm corresponding to the $S_0 \rightarrow S_2$ transition. BSA-NO has CD response from other amino acid side chains between 300-400 nm; and these signals interfere with the 335 nm band. The shape of the rotatory signal in the CD spectrum is similar to that of the absorption band although the two signals are shifted by *ca.*10 nm of one another (Figure 9.1).

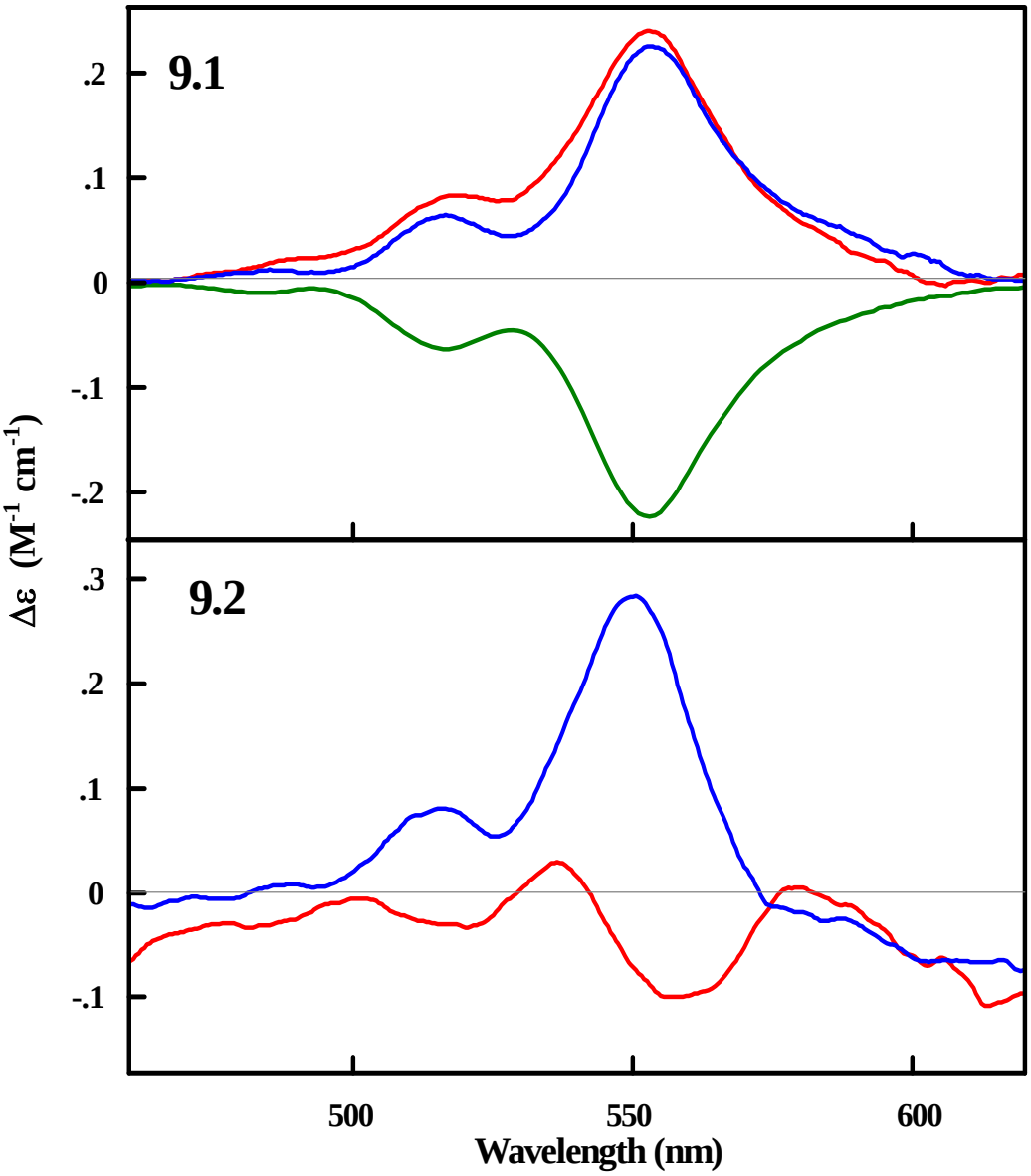

Figure 9: Circular dichroism spectra

(9.1) The uv-vis circular dichroism spectrum of L-cysteine-NO (blue), D-cysteine-NO (green), glutathione-NO (red) at pH=2.5. (9.2) Circular dichroism spectrum of BSA-NO at pH=2.5 (blue) and pH=7.0 (red).

Rotational strength, which is proportional directly to the CD signal, can originate from either $\vec{\mu} \bullet \vec{\mu}$ or $\vec{\mu} \bullet \vec{m}$ terms (Rosenfield's equation: equation 2)[31]

$$R_{i0} = \mathrm{Im}\left(\langle 0|\mu|i\rangle \bullet \langle i|m|0\rangle\right) \qquad (2)$$

When the cysteine amino acid is changed from *d* isomer to *l* isomer, the CD signal is constant in magnitude but changes in sign. This shows that the magnetooptical signal derives from the influence of the nearby chiral center environment since neither S nor N itself is a chiral center. The absence of nearby, strongly magnetic dipole-allowed transitions further suggests that the rotational strength does not derive from the $\vec{\mu} \bullet \vec{\mu}$ term but rather from the $\vec{\mu} \bullet \vec{m}$ term. When the chiral center is changed from *d* to *l*, $\vec{m}$ changes its direction by 180^{o} giving rise to the inversion of the signal. The difference in the rotational strengths in Cys-No and GS-NO may be accounted for by the differences in μ contributions.

The pH dependence of the CD signal has also been studied as shown in Figure 9.2. Only the BSA-NO shows a pH dependent signal. The 550 nm band of BSA-NO decreases, and is finally partially inverted as the pH goes from 2 to 7. It is not the magnitude of $\vec{m}$ or $\vec{\mu}$ that gives rise to the pH dependent signal but rather the change in the angle between the magnetic and electric dipole moment vectors[32] which is believed to be related to the CS-NO dihedral angle. Our temperature dependence studies of Cys-NO show that $\Delta\varepsilon$ reversibly decreases with temperature from 10 to 80 ^{o}C. Combining with the *ab initio* calculations, which predicts two minima for the cis and trans conformers, as discussed later, we conclude that as the temperature changes, the equilibrium between the two conformers change. The cis and trans conformer have roughly the same CD signal but opposite in sign, as $\vec{\mu}$ in this case has a direction change of roughly 180^{o}.

4.0 PROGRESS SO FAR

4.1 AB INITIO CALCULATIONS TO AID OUR UNDERSTANDING OF ELECTRONIC PROPERTIES

4.1.1 Model Used

S-nitrosocysteine is chosen as a representative model for *ab initio* calculations due to its affordable size.

4.1.2 Geometric optimization and potential energy surface of ground electronic state of the system

The geometry of nitrosylated cysteine was fully optimized and the single point energy is calculated by Gaussian 94 at HF/6-31(d,p). [33] The polarizable function d and p were added to the Gaussian basis set in order to better account for the sulfur atom. The starting geometry was obtained from the default amino acid cysteine template in the Spartan program (the D-enantiomer is used) with the H on sulfur being replaced by the NO group. A C-S-N=O dihedral angle of 180 ^{o} was used as an initial geometry. The detailed coordinates of fully optimized trans-cysteine-NO are included in Appendix A. The ground state single point energy of this fully optimized geometry which has the C-S-N=O dihedral angle of 179.4 ^{o}, was found to be -848.0200438 hartees or –532141 kcal/mol. This molecule has total of 39 internal degrees of freedom, and the C-S-N=O dihedral angle is of particular interest.

Schinke [34] and his cow orkers studied a sim ilar system of m ethyl thio nitrite and produced a potential energy surface cut along the S-N bond le ngth degree of freedom and C-S-N=O dihedral angle. The C-S-N=O dihedral angle is be lieved to b e the sign ificant one in controlling the confor mations of the molecules, theref ore, the PES f or the cysteine-NO was calculated using the above opt imized geometry as a starting point. The PES was scanned along the C-S-N=O only, k eeping all other coor dinates f rozen to minimize the calculatio n tim e. Figure 10 shows this potential energ y surface which reveals two well-defined m inima at the dihedral angles of *ca.*180^{o} and 0 ^{o} (trans and cis conformer), respectively. In a ddition to this prelim inary calculation o f restric ted PES, Ramachandra Kondru, a graduate student in Beratan group kindly helped to calculate a relaxed PES along the sam e coordinate with slightly lower basis set at 6-31G*. This relaxed PES (also show n in Figure 10) stil l re veals two well-def ined poten tial w ells. However, the energy of the cis confor mer reduces greatly, down close to the trans conformer energy. In addition, the barr ier between the two wells reduces to approximately 8 kcal/m ol. This is not su rprising as the relaxe d PES is obtained by scanning along the coordinate of interest a nd allowing other coordi nates to relax. In conclusion, the calculations support the use of cis and tr ans as two representative conformers.

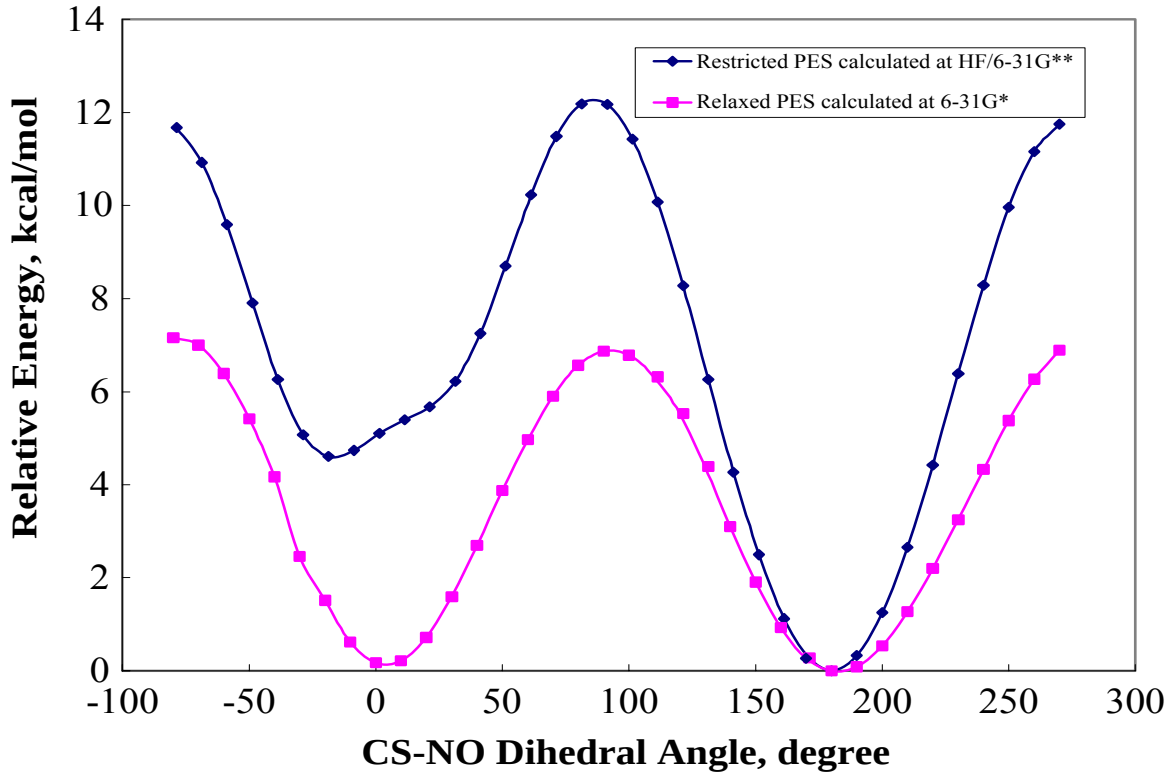

.

Figure 10: Calculated potential Energy Surface

Restricted PES along the CS-NO dihedral angle calculated at HF/6-31G** compared with the relaxed PES calculated at slightly lower level basis set HF/6-31G*. The two surfaces are put at the scale so that the lowest point lies at 0 kcal/mol. Please note that since the relaxed surface was calculated with lower basis set, its energy is about 174 kcal/mol above the restricted PES which was calculated with additional polarized basis set(6-31G**)

4.1.3 CIS calculations help understand the absorption spectra

CIS (Configuration Interaction with Singlet Ex citation Only) is an affordable calculation for calculating the excited state wavefunctions. It is a ve ry low level calcu lation as it ignores m any correlations by using only the in teractions between si nglet excitations. However, it provides basic insight into wh ich m olecular orbitals have significantly participated in the f irst two excita tions of interest. The calculations are perform ed for both cis and trans conform ers at 2 levels of basis sets, 6-31G and 6-31G**. Table 1 lists

the values of oscillator strengths of the two lowest transitions calculated at two different levels of basis sets. The $S_0 \rightarrow S_1$ has lower oscillator strength leading to the weaker band being observed in the uv-vis absorption spectra. One notable result, at both levels of basis set used, is that the cis conformer has much higher oscillator strengths for both $S_0 \rightarrow S_1$ and $S_0 \rightarrow S_2$ transitions.

Table 1: The calculated oscillator strength

Conformers	**CIS/6-31G**		**CIS/6-31G****	
	Oscillator Strength of $S_0 \rightarrow S_1$	**Oscillator Strength of $S_0 \rightarrow S_2$**	**Oscillator Strength of $S_0 \rightarrow S_1$**	**Oscillator Strength of $S_0 \rightarrow S_1$**
TRANS	0.0006	0.008	0.0005	0.0030
CIS	0.0011	0.0226	0.0007	0.028

A detailed molecular orbital analysis coupled with the excitation vectors from from the CIS calculations indicated that for both cis and trans conformer, the $S_0 \rightarrow S_1$ transition mainly involves the movement of electron density from the molecular orbital that has mostly π^* character of the NO bond into a molecular orbital that has mainly S-N-O π^* character. These two MO orbitals have similar local symmetry but they are perpendicular as shown in Figure 11, therefore, the $S_0 \rightarrow S_1$ is weak for both conformers. The $S_0 \rightarrow S_2$ transition in the trans conformer mainly involves the movement of electron density from a molecular orbital that has mostly non-bonding character on the S atom into a molecular orbital that has mainly non-bonding character on S and N (there is a little bit of σ^* character mixing in.) as shown in Figure 12 (top). The two MO's are not as perpendicular as seen in the $S_0 \rightarrow S_1$ transition so the transition is stronger as confirmed by experiment and calculated oscillator strength. The $S_0 \rightarrow S_2$ transition in the cis conformer mainly involves the movement of electron density from the molecular orbital that has mostly non-bonding character on the S atom into a molecular orbital that has mainly S-N-O π^* character as shown in Figure 12 (bottom). The $S_0 \rightarrow S_2$ transition is stronger in the cis conformer than in the trans conformer. The fact that in both $S_0 \rightarrow S_1$

and $S_0 \rightarrow S_2$, the electron density moves into the MO that has S-N anti-bonding character explains why both transitions lead to the S-N bond breaking.

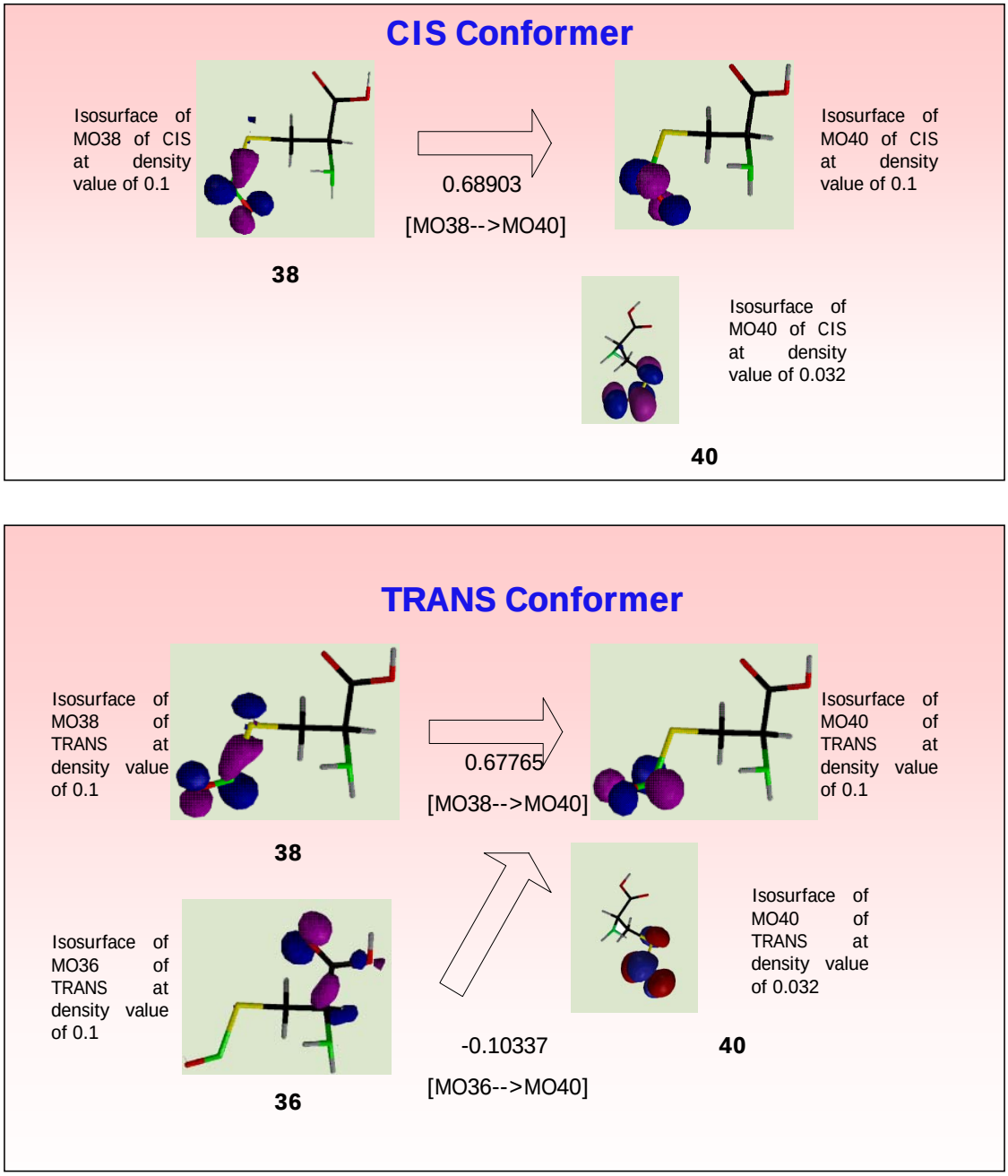

Figure 11: Molecular orbitals involving S_0 to S_1 transition

The diagram shows the molecular orbitals involved in S_0 to S_1 transition of the cis and trans conformers obtained from the CIS calculation. The number under the arrow indicates the coefficient of the interaction vector. The HOMO is MO 39 and the LUMO is MO 40. The orbitals are calculated and drawn by Spartan.[35]

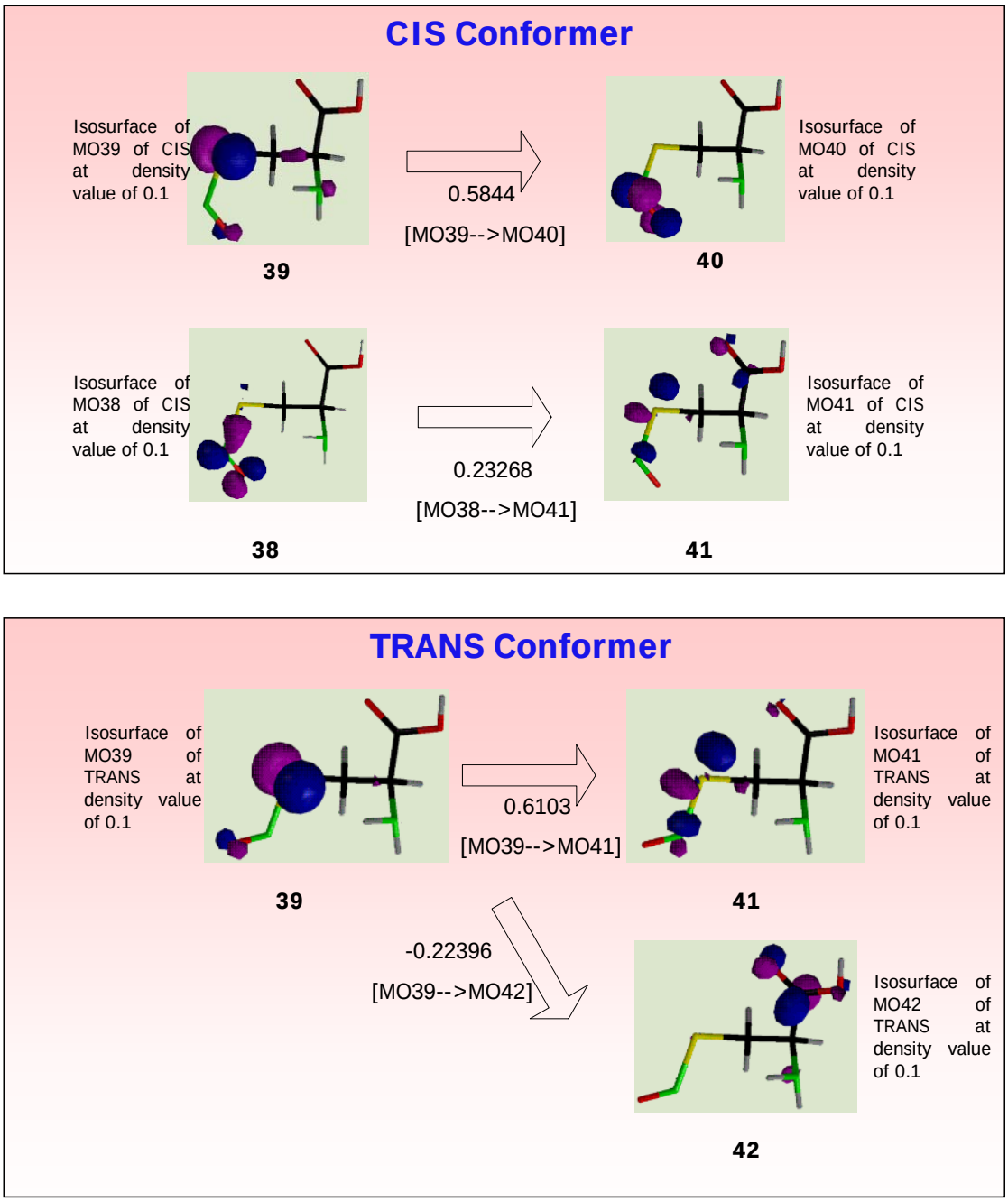

Figure 12: Molecular orbitals involving S_0 to S_1 transition

The diagram showing the molecular orbitals involved in the S0 → S2 transition of the cis and trans confor mers obtained from the CIS calculation. The num ber under the arrow indicates the coefficient of the interaction vector. The HOMO is MO 39 and the LUMO is MO 40. There are m ore orbitals involve d but only those which have the two highest coefficients of interaction vectors are shown.

The CIS calculations also yield the direction of the electric dipole moment of the transitions. This information coupled with geometry of both conformers is represented in Table 2 which shows the angles between both $\vec{\mu}_{S_0 \to S_1}$ and $\vec{\mu}_{NO}$, and $\vec{\mu}_{S_0 \to S2}$ and $\vec{\mu}_{NO}$. ($\vec{\mu}_{NO}$ refers to NO stretching dipole so this vibrational transition dipole moment is along the NO bond) These angles are important in interpreting anisotropy measurements of visible pump and infrared probe experiments, as will be discussed later. We also have predictions of the angles between the two lowest transition dipole moments and other bonds. Some of these are IR accessible as local modes, thus providing a redundant set of measurements for geometry determination to compare with theory. Comparing 6-31G and 6-31G** levels, we find that the addition of polarized functions (d function on second row elements) has very little effect on the $S_0 \rightarrow S_1$ transition whereas it has a significant effect on the $S_0 \rightarrow S_2$ transition. This signifies the lack of participation of d orbitals in the $S_0 \rightarrow S_1$ transition and a significant participation of d orbitals in the $S_0 \rightarrow S_2$ transition.

Table 2:The angles between the transition electric dipole moments of the two conformers with respect to the relevant bonds. (~local modes)

Bond	**CIS Conformer**				**TRANS Conformer**			
	S_0-->S_1		**S_0-->S_2**		**S_0-->S_1**		**S_0-->S_2**	
	6-31G	**6-31G****	**6-31G**	**6-31G****	**6-31G**	**6-31G****	**6-31G**	**6-31G****
N-C	45.32°	45.15°	61.09°	55.66°	32.7°	32.7°	61°	161.8°
C-C	110.4°	111°	16.52°	15.87°	98.76°	99.54°	71.56°	95.51°
C=O	61.4°	62.6°	39.66°	41.66°	59.95°	61.48°	106.4°	107.3°
C-O	150.2°	148.8°	83.3°	81.39°	134.2°	133.1°	49.44°	77.71°
C-C	27.95°	29.41°	93.82°	95.47°	34.65°	35.68°	119.4°	113.5°
C-S	92.4°	93.96°	71.74°	79.46°	94.02°	95.56°	151°	60.6°
S-N	87.63°	87.7°	147.6°	155.4°	87.55°	87.2°	125.4°	71.59°
N=O	88.68°	87.3°	150°	142.6°	92.43°	93.73°	168.2°	57.37°

4.1.4 Calculation of rotational strength

The calculation of rotational strength of the system was performed on conformers along a restricted potential (varying the CS-NO dihedral angle). The calculation program Dalton was used.[36] This program uses a special type of atomic orbital called London Type Atomic Orbital to avoid gauge-origin dependence of magnetic properties combining with the Random Phase Approximation.[37] The results show that the rotational strength is very dependent on the CS-NO dihedral angle as shown in Figure 13.

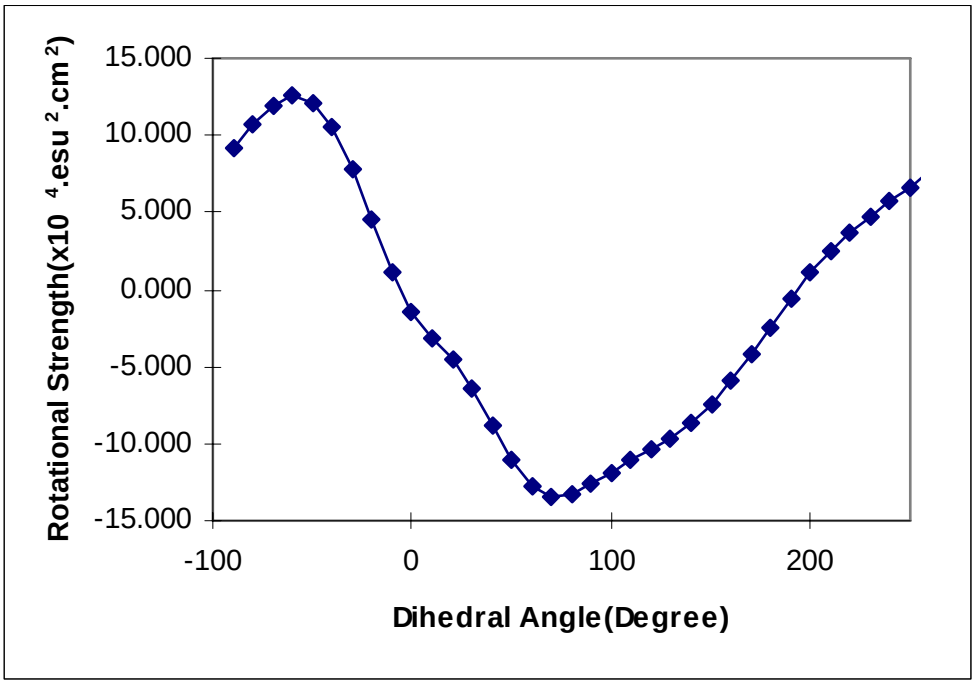

Figure 13: Calculated rotational strength as a function of CS-NO dihedral angle.

4.2 PHOTOINDUCED RELEASE OF NITRIC OXIDE FROM S-NITROSOGLUTATHIONE CHARACTERIZED BY ULTRAFAST INFRARED AND VISIBLE SPEPTROSCOPY

In this study, we have performed tim e-resolved experim ents. Photocleavage of nitrosothiols caused by the S_1 or S_2 excitation is prob ed in the in frared to re veal population and relaxation dynamics for both the NO and the parent peptide.

4.2.1 Experimental Method

GSH was obtained from Sigma (St. Louis), D_2O is obtained from Cambridge Isotope, and all other chemicals are obtained from Aldrich. They were used without further purification. GSNO solution was prepared by dissolving required amount of GSH into either H_2O or D_2O (D_2O was used for IR probe measurement). The solution was then acidified with HCl or DCl until the pH is *ca*. 3-4. Then an equimolar amount of $NaNO_2$ solution was added and the mixture was stirred for 20 to 30 minutes. The volume of the solution was then adjusted to obtain the desired concentration. When a stream jet was used in the time-resolved measurements, the pH of the solution was adjusted to ca. 7-8 with NaOH before the volume was adjusted.

The 400 nm pump/400 nm probe measurements were done at 180mM GSNO concentration in a 1mm pathlength flowing cell. The 400 nm pump/IR probe measurements were done at 500 mM in a 100 μm pathlength CaF_2 flowing cell or in a 100 μm thick free jet. Flowing the sample prevented detrimental burning/bleaching of the sample and provided a fresh sample volume for each laser pulse. It also eliminated problems from NO and/or O_2 bubbles which formed in a closed, spinning sample cell.

The time-resolved data were collected using a pump-probe technique, pumping with 400nm which was an ultrashort light pulse generated from a solid-state Ti:sapphire system, combined with parametric light amplification techniques. Probe pulses were either 400nm or a tunable IR probe which was generated using optical parametric amplifier (OPA) and different frequency generation (DFG). A detailed description of the

laser and optic systems used for generation of pump and probe pulses can be found elsewhere.[38] ΔOD is the absorbance measured by the laser probe pulse in the presence of the excitation pulse minus the absorbance measured by the probe pulse in the absence of the excitation pulse. The time profile was controlled by the variable delay stage with delay the pump pulse to reach the sample at various times either before or after the probe pulse. A multi-exponential functional form, $\Delta A(t) = \sum_i A_i \exp(-t/\tau_i) + c$, was fit to the data. The apparatus was as shown in Figure 14.

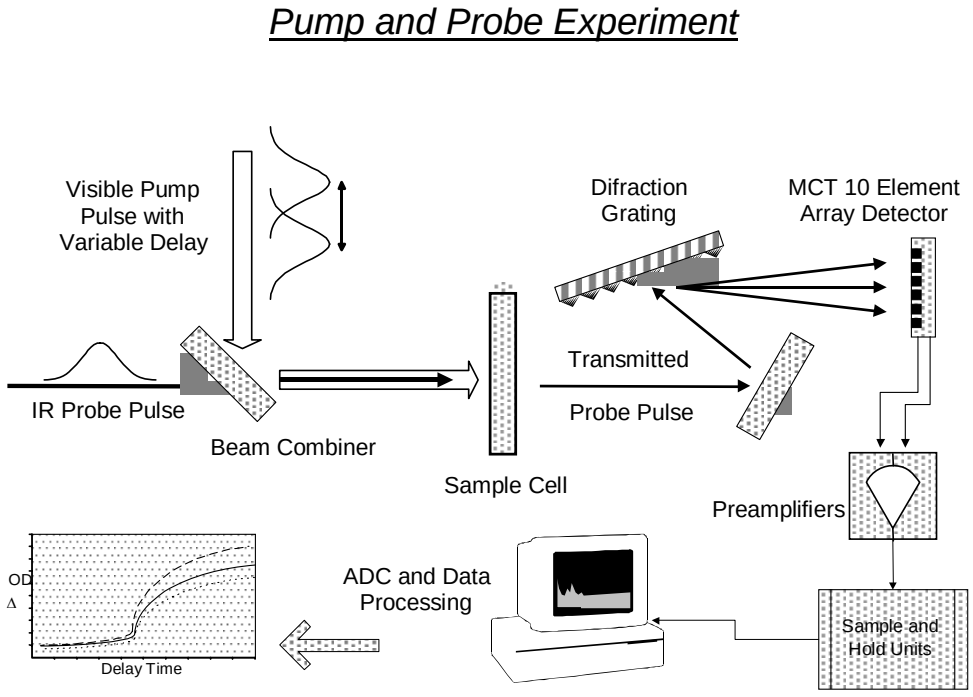

Figure 14: Schematic of pump/probe apparatus

The apparatus is for collection of time-resolved transient spectra. Please note that for 400 nm pump/400 nm probe, the probe beam is directed directly into a photodiode without passing through the monochromator grating.

4.2.2 Results and Discussion

4.2.2.1 400 nm pump/IR probe: In the 400 nm pump/IR probe experiment on GSNO, we observed bleaching of the NO stretch in S-NO chromophore and geminate recombination. Figure 15 shows the spectral kinetics in the NO stretch region(1528 cm^{-1}). The induced transmission (bleach) signal is seen to recover on two time-scales, 2.6 and 30 ps, respectively. The data do not show a significant time-dependent frequency shift. The early time bleach amplitude is consistent with the excitation energy, 1 microjoule, and indicates that the earliest signal corresponds to loss of NO. The 2.6 ps component appears to be caused primarily by geminate recombination, with additional contributions from thermal relaxation; the longer 30 ps component is dominated by thermal relaxation, corresponding to cooling of low frequency modes of the nearby solvent molecules. The ground state cross section of GSNO at 1530 cm^{-1} decreases by 0.7%/K as temperature increases.

The gas phase NO absorbs around 1870 cm^{-1},[39] while the NO radical in water absorbs around 1835 cm^{-1}.[40] Figure 16 shows the formation of the solvated NO species in ca 2.7 ps. Detection of this species is novel. There is no evidence of NO vibrational relaxation, consistent with gas phase photocleavage of methyl thionitrite.[34] The solvation process for the NO radical is not pronounced in the transient IR spectra, although there is detectable transient absorbance between 1870 and 1835 cm^{-1} within the first several picoseconds which may arise from solvation.

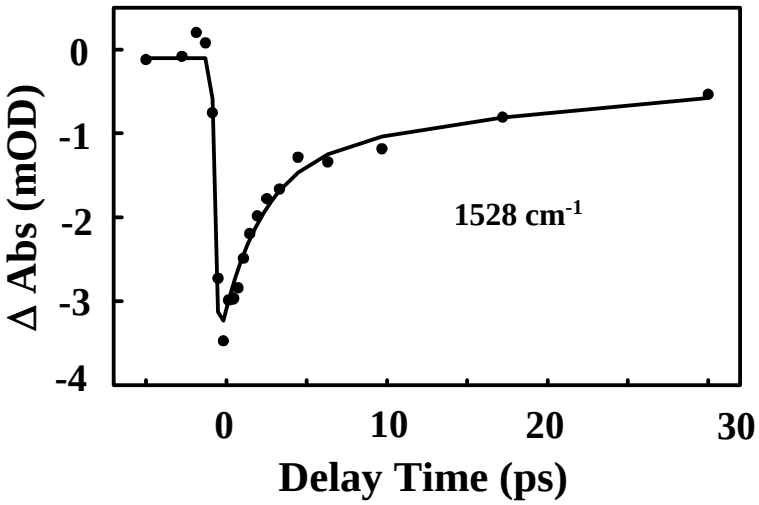

Figure 15: The absorbance change kinetics at the 1528 cm^{-1}

The frequency is corresponded to the center of the NO stretch band of GSNO. It exhibits a subpicosecond bleach caused by NO loss and a 2.6 ps recovery correspond ing to geminate recombination and cooling.

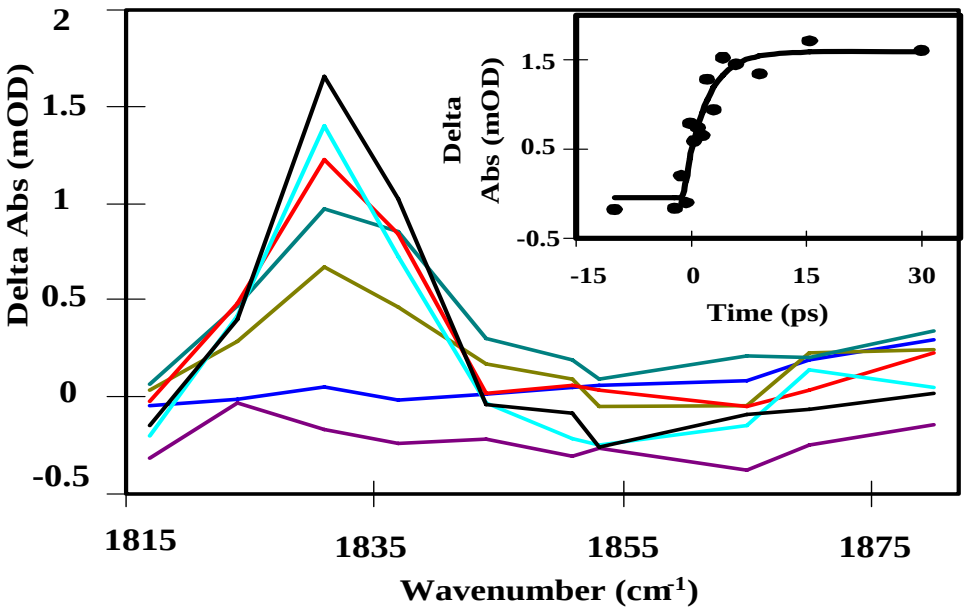

Figure 16: The time-dependent spectra in the region of 1815-1875 cm^{-1}

They reveal the formation of solvated NO radical. The lines correspond to the photoinduced difference spectra at –6.0, - 1.0, 0.6, 1.8, 3.5, 7.4 and 22.7 ps, respectively. The 1831 cm^{-1} band (th e inset) app ears with a 2.7 ps tim e constant as illus trated in the transient data and corresponding fit.

The process of NO solvation is likely to be dominated by hydrogen bonding with water molecules. The 2.7 ps is the average time required for the photocleaved NO to migrate to the first solvation shell and reorient for hydrogen bonding. This process is similar to the trapping of CO by a nearby docking site once it is photocleaved from the heam in myoglobin.[41] Although free rotation of NO occurs on a time-scale of $(kT/I)^{1/2}$ (~200 fs), prior association of NO with one water molecule cause the reorientation time to be ca 1-2 ps if single hydrogen bond dynamics dominate the process.[42] Future examination of the solvent and parent dependence of the rebinding rate will test this simple model, which neglects details of the photocleavage environment.

4.2.2.2 400 nm pump/400 nm probe: We have also performed 400nm pump/400nm probe studies of the kinetics of the optically prepared electronic states. These data are shown in Figure 17. The data exhibit a positive induced absorbance that rises in *circa* 1 ps and decays with *ca* 300 ps. From Figure 6, we can see that the ground state absorbance at 400 nm is 170 cm^{-1} M^{-1}. From the transient data we can estimate that the photoinduced species that is formed has a cross section of ca 500 M^{-1} cm^{-1} assuming that it corresponds to the photocleaved parent. The literature value for the equilibrium cross section of the GS• is ca 150 cm^{-1} M^{-1} at 400 nm.[43] On this basis we conclude that the absorbance we find is not caused by the thiyl radical absorbance.

The dominant photodynamic process is geminate recombination. The temperature dependence of the $S_0 \rightarrow S_2$ transition dipole strength at 400 nm of GSNO is less than 0.2%/K (data not shown), and therefore the signal is not caused by a sample of Boltzman distributed but by warm ground state species. We suggest that the larger fraction of photocleaved molecules subsequently recombine in a metastable conformation. As mentioned earlier, our preliminary calculations indicate that the $S_0 \rightarrow S_2$ transition in the higher energy cis conformer has significantly greater dipole strength than the trans conformer. The decay of the absorbance may then be interpreted to correspond to barrier crossing to the global minimum energy geometry. Whether the cis-trans isomerization is the correct ground state relaxation process is the subject of ongoing studies.

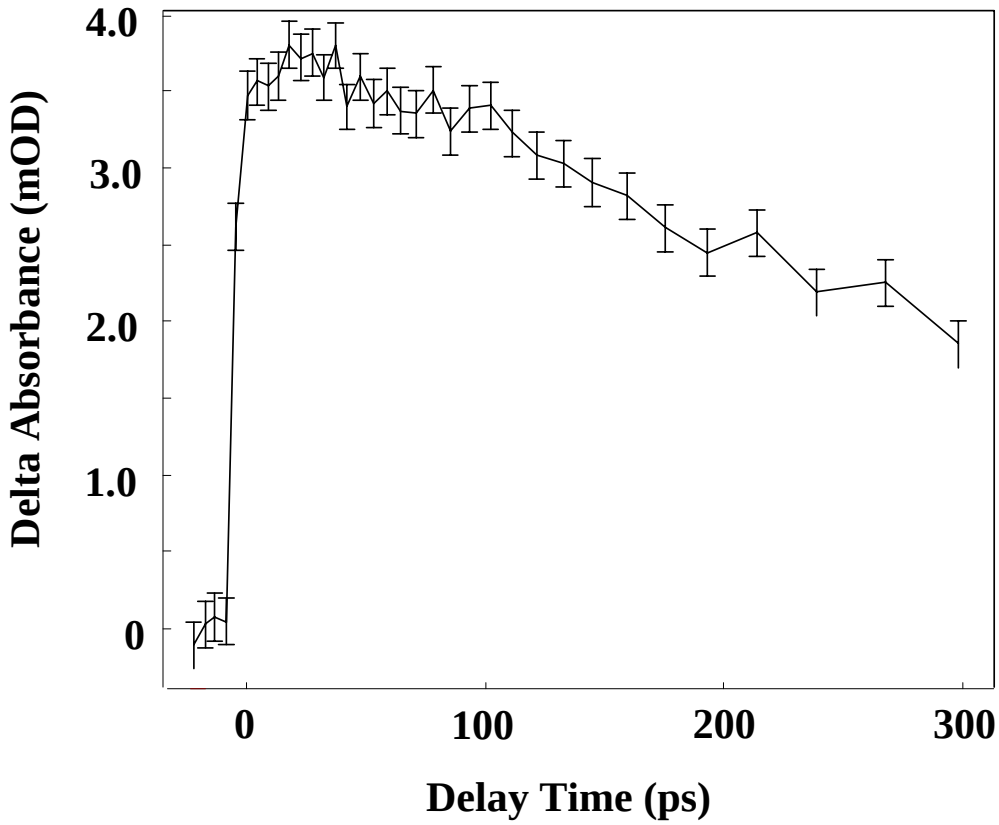

Figure 17: 400 nm pump/400 nm probe transient spectrum of GSNO

The time-dependent photoinduced absorbance of GSNO as measured by 400 nm photolysis and 400 nm probe pulses is shown in the transient data. The induced absorbance that appears in 1 ps and survives with a ca. 300 ps lifetime is attributed to a metastable conformer of geminately rebound GSNO.

4.2.2.3 Anisotropy measurements: Anisotropy measurements[44] were made to determine the relative direction of pumped and probed transition dipole moments. These measurements for 400nm pump and 1522-1580 cm^{-1} probe at 10 ps delay showed a single anisotropy of ca 0.26 $\pm$ 0.04 corresponding to an ensemble averaged angle between the electronic and vibrational transition dipoles of *ca* 30^{o}. This angle should be roughly

corresponds to th e angle between $\vec{\mu}_{S_0 \rightarrow S_2}$ and $\vec{\mu}_{NO}$. Before the pum p, the two conformers therm ally populated and since the trans conform er is lowe r in energy, this conformer is expected to dom inate the phot oexcited population. However, based on our previous assumption, these excited molecules wi ll geminately recombine preferentially in the cis con former. T herefore, th e best ca lculated angle to b e co mpared with this experimentally determ ined anisotropy is the angle between $\vec{\mu}_{S_0 \rightarrow S_2}$ of the trans conformers and $\vec{\mu}_{NO}$ when t he two m olecules are overlay ed on top of each other. The obtained angle is *ca*. 39 °. Anisotropy m easurements m ade at 400 nm pum p/400 nm probe reveal a tim e de pendent anisotropy is *circa* 0.2 ± 0.04 between 0.4 and 3 ps. Assuming that this signal is due to both the anisotropy of the bleach and a new single absorbing species (e.g., the cis conform er), we conclude that the new species has an $S_0 \rightarrow S_2$ transition moment that is at a *ca* 45° angle relative to the originally excited transition.

The sim plest angle calculated from our theoretical work that will roughly represent th is anisotropy value is th e angle between $\vec{\mu}_{S_0 \rightarrow S_2}$ of the trans conform er and $\vec{\mu}_{S_0 \rightarrow S_2}$ of the cis conformer. This calculated angle is 1 07°. The discrepancy between the calculated values and the experimental values may arise from several factors. First of all, the whole population before th e excitation is not all in the trans conform er, unlike the calculation. Furtherm ore, the m olecules undergo rotation, therefore the calculated angle assumes the orienta tion of all o ther parts of the molecule to be s tationary in s pace a fter excitation u ntil the rec ombination which is unrealistic. In orde r to im prove our theoretically calcu lated angle, th e energy diffe rence of the two conform ers needs to be included so that the therm al distribution can be accounted for. In addition, the m olecular rotational tim es have to be includ ed so th at the calculated a ngle may be used to accurately represent what happens in the real sy stem. Moreover, the calculation sho uld be perform ed at higher level such as MCSC F which allows m ore configurations to interact. T hese are all im provement that will be undertaken. W hile the calculation is being im proved, the an isotropy m easurements will be expanded as well to im prove the experimental characterization.

4.3 INVESTIGATION OF POSSIBLE MIGRATION OF NO GROUP FROM CYSTEINE-34 TO OTHER AMINO ACID RESIDUES OF BOVINE SERUM ALBUMIN AFTER PHOTOCLEAVAGE OF S-NO

In this preliminary work, several UV-Vis and fluorescence spectra of nitrosylated BSA solution at pH *ca*. 3 and 8 were taken before and after irradiation by the YAG laser at 527 nm which causes the $S_0 \rightarrow S_1$ transition. As a result of the excitation, the S-NO bond cleaves and NO· is released. The question being raised here is "where does this NO· go?" Stamler has shown that 90% of the NO· radicals that cleave out make a geminate recombination.[15] What is about the other 10%? If that 10% just come off and goes into solution, then we would expect only a small local alteration around the loop between helix 2 and helix 3 where Cys-34 resides due to the loss of NO and we would expect to see mainly bleach bands of $S_0 \rightarrow S_1$ and $S_0 \rightarrow S_2$ centered at 550 nm and 335 nm respectively in the spectral range above 300 nm. However, if this is not the case and some of the cleaved NO migrates to other amino acid residuals and nitrosylates them, then the BSA molecule could be altered functionally. For example, if tyrosine residual is nitrosylated and becomes 3-nitrotyrosine, the most stable form of nitrosylated tyrosine, then it can becomes a marker for protein catabolism.

4.3.1 Experimental Method

BSA (98%), GSH (98%), and L-Cysteine (98%) were obtained from Sigma (St. Louis). Other chemicals are from Aldrich (St. Louis). They were used without further purification

Bovine Serum Albumin solution was prepared by dissolving solid BSA into 100 mM EDTA degassed solution to make about 1 mM BSA solution. The S-nitrosoBSA was synthesized following Stamler's method.[20] First the pH of the solution was adjusted to *ca* 2.7. by adding HCl. An equimolar amount of 50 mM $NaNO_2$ solution was added, and the mixture was stirred at room temperature for 30 minutes. For the pH 8 solution, NaOH or

KOH were used to adjust the pH. The prepared solutions were usually kept in dark and used within 2 hours.

Irradiation was done using the 527 nm light from a frequency doubled Nd-YAG laser (Quantronix). The beam was passed through samples that are stirred in 1 cm cells. Uv-vis spectra were collected after various irradiation times. Fluorescence spectra were collected after 30 minutes irradiation.

The UV Visible spectra before and after irradiation were measured using a Diode Array Hewlett Packard Spectrophotometer Model 8451. The difference spectra are obtained by subtracting the spectrum before irradiation from the spectrum after irradiation. The spectrum of the dark control, which is obtained by taking the spectra of the sample kept in dark for the same period as irradiation period, was subtracted out to exclude thermal decomposition products. The similar spectrum was also obtained for the case of BSA solution.

4.3.2 Results and Discussion

4.3.2.1 Is it really $NO^{\cdot}$ that comes out of the protein after the photocleavage?: In small S-nitrosothiols species such as S-nitrosocysteine, S-NO bond photocleaves and yields thiyl radical and NO radical. However, in the BSA-NO system, the pKa of thiol is lower than the free thiols, and it may be that photocleavages of the S-NO bond cleavage leads to the formation of thiyl anion and NO^{+}. Wood and his co-workers, who measured millisecond transient uv-vis spectrum of the BSA-NO solution, did not observed the $NO^{\cdot}$ radical released into the bulk solution so they concluded that either NO^{+} is released instead of the $NO^{\cdot}$ radical or the released $NO^{\cdot}$ reacts at another site in the protein before reaching the bulk medium.[45] NO^{+} can recombine with thiyl anion or it can escape the protein pocket and become available as nitrosating agent for other amino acid residues. As we are not certain whether the photoreleased species is NO^{+}, $NO^{\cdot}$ or both, we refer to it hereafter as NO^{x}.

4.3.2.2 What do the different UV-Vis spectra tell us?: Figure 18 shows the difference spectrum of the BSA-NO solution at pH 8 revealing a bleach band centered around 350 nm and a small absorption band at *ca* 410 nm which has a shoulder extending to *ca* 500 nm. The difference spectrum of BSA solution shows no change between 200 to 250 nm (data not shown) indicating that irradiation did not significantly affect the protein backbone. The difference spectrum of the BSA-NO solution at pH 3 shows a larger bleach band centered around 350 nm but there is no apparent absorption band at 410 nm. The center of both bleach bands is not at 336 nm, as one would expect for the S-NO bleach. This indicates that there has to be a new species that absorbs significantly at 330 nm and causes the bleach band to shift.

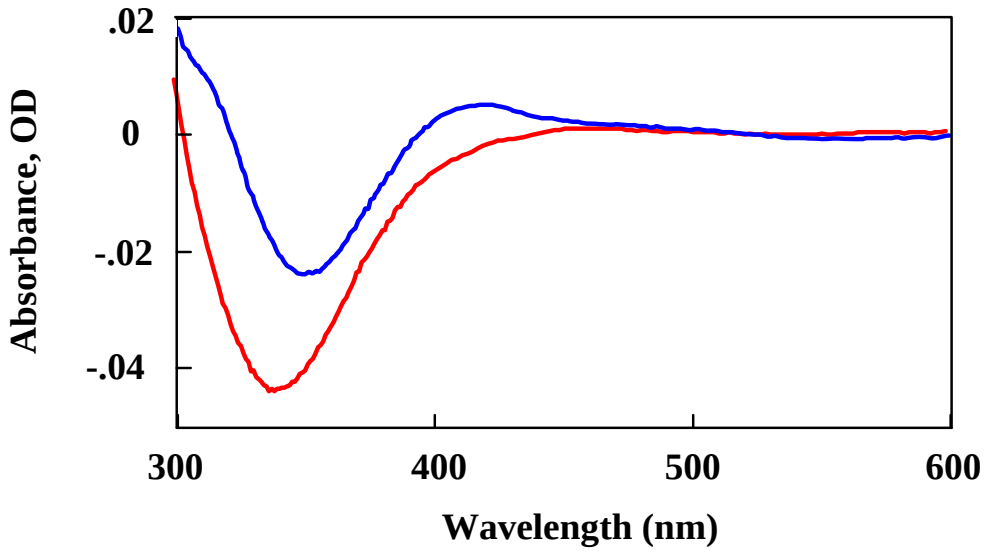

Figure 18: The difference spectra of the BSA-NO solution before and after irradiation at two difference pHs, 3 (red) and 8 (blue)

4.3.2.3 Which amino acid residuals are most likely to harbor the photocleaved NO?: We now examine the protein for site that may be attached by NO^x. Aromatic amino acids are most likely to be nitrosated through electrophilic addition of NO^x. Aliphatic residues usually do not exhibit spectral transition in the visible wavelength region. Candidates for nitrosation therefore include tyrosine, tryptophan, and phenylalanine.

Phenylalanine has been shown by others[46] and us to be non-reactive to nitrosation using either $NOBF_4$ or acidified $NaNO_2$. Thus, we exclude potential nitrosation products of phenylalanine even though there are two phenylalanine residues nearby cys-34 in the NO binding pocket. Therefore, we are left with two more aromatic residues most likely to be nitrosated, tyrosine and tryptophan.

4.3.2.4 Fluorescence spectra before and after irradiation show tryptophan is an unlikely site as there is no observable perturbation of the residues: Tryptophan by itself was found to react with sodium nitrite in aqueous acidic solution to give the nitroso derivative in which nitrosation has occurred at the indolic nitrogen.[29] However, in BSA there are only two tryptophans at the 134 and 214 positions. The closest one, which is tryptophan 134, lies 20 Å away; tryptophan 214 lies even further away at 35 Å. It is unlikely that the photoreleased NO from cys-34 will travel through the protein that far without first reacting with a closer site such as tyrosine. To check whether tryptophan residuals have been perturbed by the photorelease of the NO or not, the fluorescence spectroscopy is used. Fluorescence spectroscopy can be used as a tool to monitor tryptophan chromophores in most proteins, especially when tyrosine residues are excluded by exciting at wavelengths longer than 296 nm. In this experiment, the emission spectra of BSA solution at pH ca. 7.4 were obtained before and after irradiation as shown in Figure 19. We found the emission intensity increases after irradiation. In another experiment, when tryptophan is nitrosylated, the fluorescence intensity reduces greatly as shown in Figure 20. Therefore, if any tryptophan residue is the site being nitrosylated after the photocleavage of NO from cys-34, we would expect to see an observable decrease in fluorescence intensity after irradiation which we do not. This

indicated that tryptophan is unlikely to b e nitro sated as a con sequence o f the photocleavage.

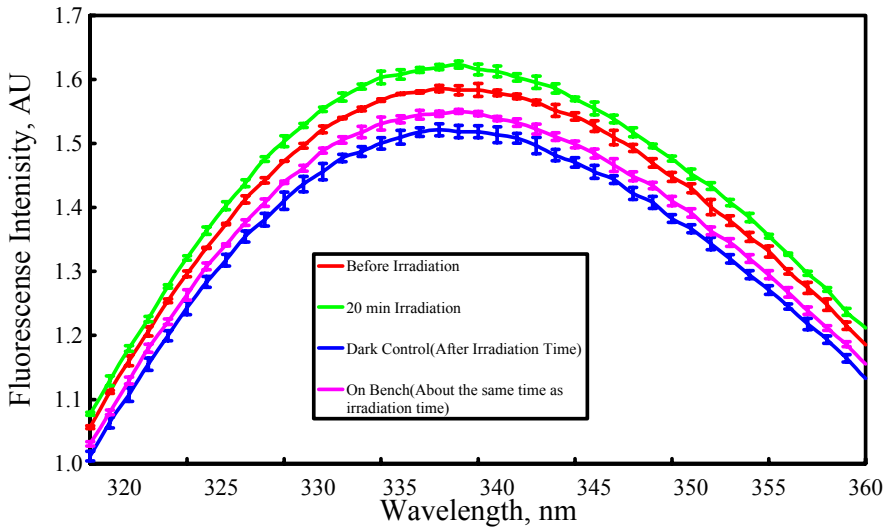

Figure 19: Fluorescence spectra of BSA-NO solution at pH 7.4

The spectra were taken before and after irra diation. Also shown are the dark co ntrol spectrum and the spectrum of the solution left under room light. The error bars show the standard deviation based on three measurements.

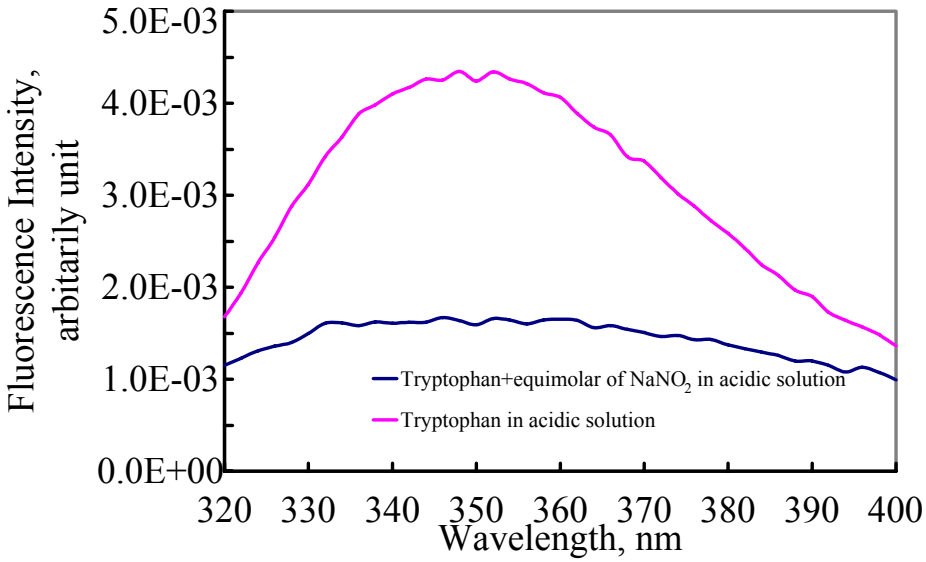

Figure 20: Comparison of fluorescence spectra of tryptophan and its nitrosylated form

4.3.2.5 Is tyrosine residual nitrosated? : Based on its prevalence BSA (15 tyrosine residuals) and its position inside the binding pocket near Cys-34 (see Figure 4), tyrosine has a high potential to be an accepting site of photoreleased NO^x. Possible nitrosated products of tyrosine include 3-nitrotyrosine, 3-nitrosotyrosine and O-nitrosotyrosine. Figure 21 shows how these products can be obtained. Furthermore, 3-nitrosotyrosine can react with nitric oxide to give 3,4-dihydroxyphenylalanine (dopa). The electronic properties of 3-nitrotyrosine are well characterized. It has a band at 360 nm (2790 $M^{-1}cm^{-1}$) in an acidic solution and a band at 427 nm in basic solution (4100 $M^{-1}cm^{-1}$).[29] We do not see any induced absorption band centered at 430 nm which leads us to the conclusion that 3-nitrotyrosine is not directly formed as a consequence of the photoexcitation. However, we are still left with 3 more products (3-nitrosotyrosine, O-nitrosotyrosine, and dopa) whose electronic properties have not been as well characterized as 3-nitrotyrosine. The formation of these products and their subsequent transformations are under further investigation.

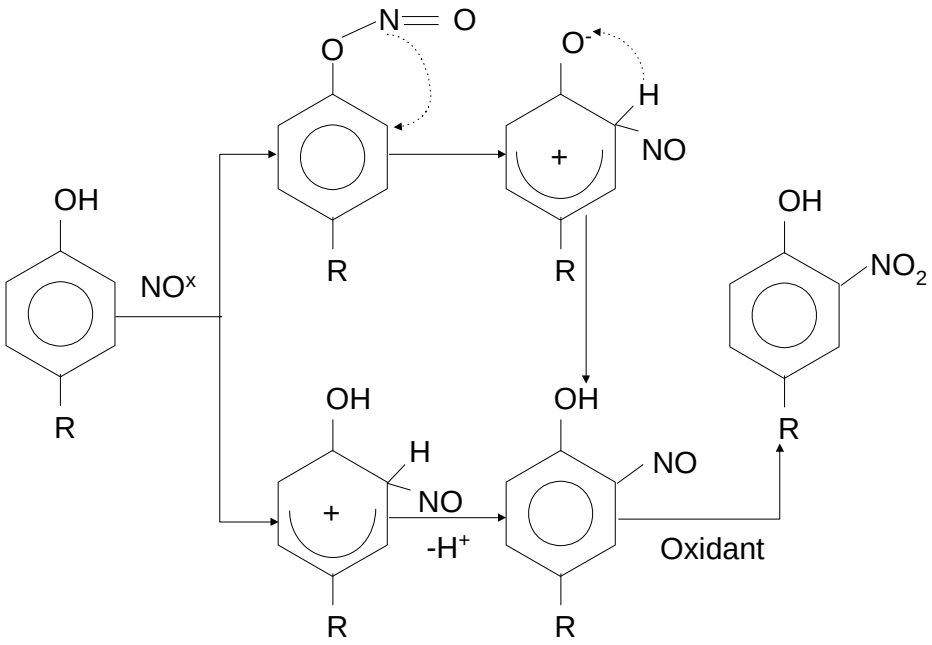

Figure 21: Nitrosation pathway of tyrosine

4.3.3 Conclusion

We are still investigating the species or chromophore that is responsible for the new absorption band at 400 nm.

5.0 FUTURE WORK

5.1 BUILDING OF TRANSIENT CIRCULAR DICHROISM TO MONITOR THE CONFORMATIONAL CHANGE OF PROTEINS AND PEPTIDES AFTER THE PHOTOCLEAVAGE OF S-NO AND THE GEMINATE RECOMBINATION

5.1.1 Goals

- To use the transien t circular dichro ism to monitor the tim e course of confor mational change of S-NO after the photoexcitation.
- To test the hypothesis that there exists a preferred direction from whi ch the NO geminately recombines with its pare nt peptid e or protein, and that it is this pref erred conformation that give rise to the induced abs orption se en in th e tra nsient lin ear absorption spectrum of GSNO. If t here is a preferred direction, i.e. cis, at which the NO recom bines, we would expect to see a transient circular dich roism signal as a result of this and th is signal wo uld decay as there sho uld be a confor mational relaxation to reach thermal equilibrium.

5.1.2 Background

Transient circular is a pow erful tool for monitoring th e secondary, tertiary, and quaternary structural relaxa tion of biological m acromolecules after a pertu rbation induced by a photoexcitation. There have been a very fe w works on transient circular dichroism especia lly in the tim e sca le sho rter than nanosecond due to its need for high sensitivity and stability of the system (the transient CD signal is usu ally very small). Lewis and Kliger are the m ain pioneers of transient circular d ichroism taken fro m

nanoseconds to seconds.[47-49] Their technique is based on the change in ellipticity of the probe beam after passing through the sample. Xie and Simon at UC San Diego were the first and only group to build a system that is capable of measuring the spectrum in the picosecond time scale.[50] However, their technique is based on direct measurement of the difference in the absorption of the left and right circularly polarized light. The time resolution is limited mainly by the pulse width. They have used their apparatus to study the protein conformational relaxation following photodissociation of CO from carbonmonoxymyoglobin[51], and photosynthetic reaction centers from *Rhodobacter sphaeroides*.[52]

5.1.3 Method

Our design is modeled after that of Xie and Simon.[47] For the transient linear absorption spectroscopy, we would need only 2 probe pulses to get the difference signal when there is a pump pulse and when there is not. However, to measure the transient circular dichroism, we need 4 probe pulses to obtain the signal as $(A_{PL}-A_{PR})-(A_{UL}-A_{UR})$ where A_{PL} and A_{PR} are the signals when there are pump pulses and the sample is probed with the left and right circularly polarized pulses, respectively, and A_{UL} and A_{UR} are the signal when there are no pump pulse and the sample is probed with the left and right circularly polarized pulses respectively.

The experimental plan is to probe the conformation of the S-NO when the NO geminately recombines after the photodissociation. We have previously characterize the well isolated CD band centered at 550 nm and shown that the CD signal depends on the conformation of the S-NO chromophore (whether it is cis or trans), therefore we will probe the system in the wave length region of this band. The signal will be too small if we excite $S_0 \rightarrow S_2$ due to the large difference in extinction coefficients. Hence, we will pump the system using the $S_0 \rightarrow S_1$ band.

5.1.4 Design of apparatus

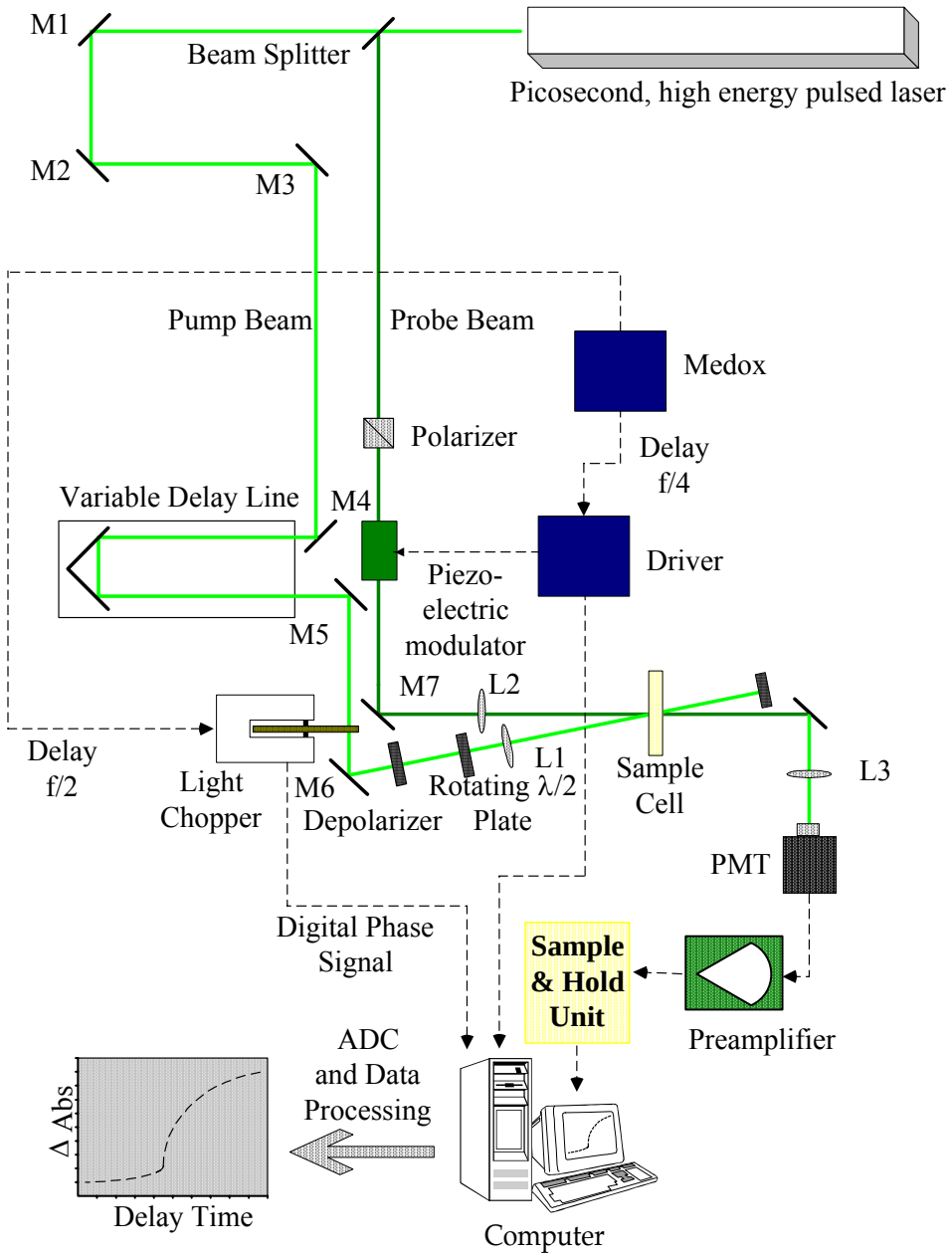

Figure 22: The proposed transient CD apparatus

The diagram for the experimental apparatus is shown in Figure 22. We will use a commercially available Nd-YAG laser that is capable of producing a pulse at 532 nm with energy higher than 1 mJ and the width less than 100 ps with the highest repetition rate possible. From the laser source, we pass the beam to the beam splitter which is a mirror that have about 20%:80% reflection to transmission ratio in order to separate the beam into the pump beam (the transmitted beam ~80% of the power of the original beam) and the probe beam (the reflected beam ~20% of the original beam) The pump beam will be directed by mirrors M1 to M4 into a variable delay stage which will allow the optical pathlength of the pump beam to be changed and allow us to collect a signal as a function of this variable delay time. After the delay stage, the pump beam is directed by a mirror M5 and passed through a mechanical chopper. The chopper exists to block every other two pump pulses so that we are able to obtain the signal when there are no pump pulses (A_{UL} and A_{UR}). After the chopper, the pump beam strikes mirror M6 which will direct the pump beam to intersect the probe beam at the angle of about 10 degree at the sample. After the mirror, the pump beam is passed through two important optics, the depolarizer and rotating half-wave plate. These two optics remove any unwanted pump induced linear dichroism contributions to the detected signal as shown by Simon and Xie using Jones matrix. After the two optics, the pump beam is focused into the sample to obtain the beam diameter of ca. 50 – 100 microns (the smaller the beam, the bigger the detected signal). The probe beam then will be passed through the polarizer to linearly polarize the beam. Then it will be passed through a piezo-electric modulator which will create a sequence of left and right circularly polarized pulses. A clock regulates the chopper and the modulator. After the modulator, the probe beam will be passed through mirror M7 in order to direct the beam into the focusing lens L2. The probe beam is focused into the sample and when it pass out, it is directed by mirror M8 to a collimating lens L3 before it reaches the photo diode. The signal from the photo diode will then be amplified by preamplifier before it is

sent to the sam ple and hold unit. Fi nally the signal will pass throu gh the analog to digital converter and data will be processed by a computer.

5.1.5 Prediction of the signal

In order to get an insight in to how big the signal that we are looking for, an initial signal has been predicted based on several assumptions and known:

- Nitrosylated glutathione exists m ainly in two confor mations, one with the trans orientation of the S-NO bond and the other with the cis orientation.
- Potential E nergy calculations of the tw o confor mers coupled with the steric consideration yield the trans conformer to be lower in energy for the GS-NO system.
- The calcu lations of electric tran sition di pole m oment and magnetic dipole m oment predict the opposite sign w ith approxim ately equal m agnitude for the rotational strength (which is proportional to the CD signal) of these two conformations
- The temperature dependent circular dichroism predicts the energy gap between the cis and trans conformers to be about 3100 cal/mol
- When GS-NO is excited either f rom S_0 to S_1 or S_0 to S_2, the S-NO bond is cleaved and $NO^{\cdot}$ is released. W ithin 1 ps, ap proximately 95% of releases $NO^{\cdot}$ recombines. In this model, we assum e the preferred orientation for the gem inate recombination is cis (assume all that recombine do so into the cis conformation).
- The lin ear cross s ection of the cis and tran s con formations are v ery sim ilar for 55 0 nm band with the ratio of ca. 7:5 (see calculation section)
- Assuming the following parameters,

– Overlap pathlength: 500 micron

– Pump beam diameter: 100 micron

– Pump wavelength ~530 nm

- Probe wavelength ~530 nm
- Cross section at pump wavelength ~12 $M^{-1}cm^{-1}$
- Cross section at probe wavelength ~12 $M^{-1}cm^{-1}$
- $\Delta\varepsilon$(rotational strength) at RT ~0.1 $M^{-1}cm^{-1}$
- RT~25 degree Celsius
- Concentration of GSNO=1M

We can calculate the signal as a function of pump energy as shown in the Figure 23.

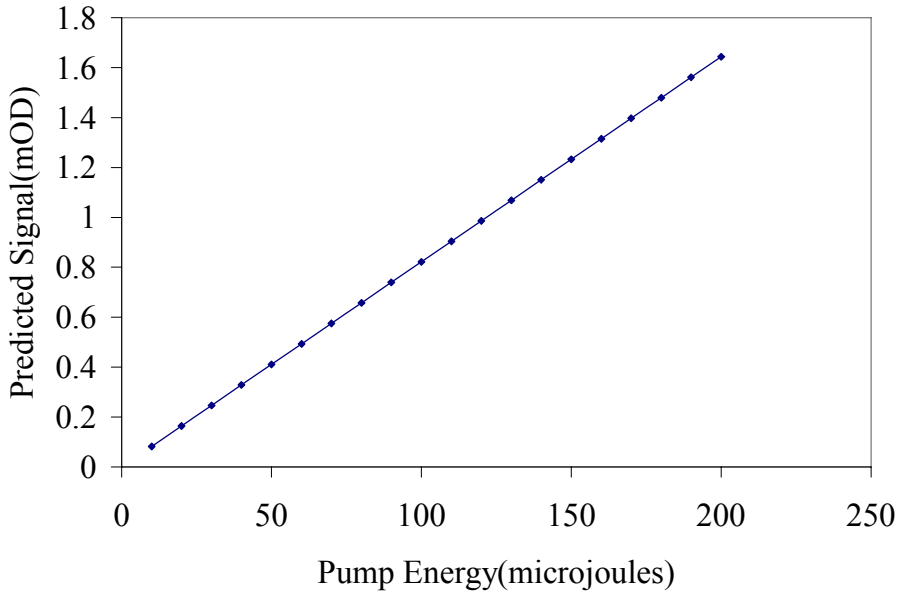

Figure 23: Predicted CD signal as a function of the pump energy.
A 100 ps pulse will be used.

5.2 CONTINUATION OF INVESTIGATION OF HARVEST SITES OF NO AFTER PHOTORELEASE IN THE SYSTEM OF SERUM ALBUMIN

So far we have used only uv-visible spectroscopy and fluorescence spectroscopy to investigate the potential site for binding photoreleased NO. These two techniques provided us some useful information. Nevertheless, they cannot provide enough evidence to make any concrete conclusion. To further investigate this we will try the followings:

- Hydrolyze sample of BSA-NO solution before and after irradiation and use chemical separation technique such as HPLC to separate the components and compare them between before and after irradiation.
- Use ^{15}N NMR spectroscopy as a tool to identify the site. We will nitrosylate the protein with Na $^{15}NO_2$ and obtain the ^{15}N NMR spectra before and after irradiation. Different environments around ^{15}N will lead to different chemical shift. We expect to see a decrease in a peak corresponding to cys-^{15}NO and an increase in a peak corresponding to the formation of new species as a result of irradiation.

ACKNOWLEDGEMENTS

I thank my advisor, Prof. Gilbert Walker, for his supervision. I also thank my colleagues, Chengfei Wang who ki ndly set up m ost of the pum p-probe apparatus and Brian K. Mohney for his kind help with collecting the static difference spectra and sharing his great knowledge in various fields.

REFERENCES

[1] Crutzen, P.J. "The influence of nitrogen oxides on the atmospheric ozone content", *Quart. J. Roy. Meteor. Soc*., **1970**, 96, 320-325.

[2] This discovery led Paul Crutzen to his Nobel Prize in Chemistry in 1995.

[3] McDonald, L. J.; and Murad F. "Nitric oxide and cyclic GMP signaling", *Proc. Soc. Exp. Biol. Med*., **1996**, 211, 1-6.

[4] Furchgott R. F. The 1996 Albert Lasker Medical Research Awards. "The discovery of endothelium-derived relaxing factor and its importance in the identification of nitric oxide", *Jama*, **1996**, 276, 1186-1188.

[5] Ignarro, L. J.; Buga, G. M.; Wood, K. S.; Byrns, R. E.; and Chauduri, G. "Endothelium-derived Realxing Factor Produced and Realeased from Artery and Vein Is Nitric Oxide", *Pro. Natl. Acad. Sci*., **1987**, 84, 9265-9269.

[6] Dawson, V. L.; and Dawson T. M. "Physiological and toxicological actions of nitric oxide in the central nervous system", *Adv. Pharmacol*., **1995**, 34, 323-342.

[7] Garthwaite J.; and Boulton C. L. "Nitric oxide signaling in the central nervous system", *Annu. Rev. Physiol.*, **1995**, 57, 683-706.

[8] De Groote, M.A.; Testerman, T.; Xu, Y.; Stauffer, G.; Fang F. C. "Homocysteine antagonism of nitric oxide-related cytostasis in Salmonella typhimurium", *Science*, **1996**, 272(5260),414-417.

[9] Granger, D. L.; Hibbs, J. B. Jr. "High-output nitric oxide: Weapon against infection?" *Trends in Microbiology*, **1996**, 4(2), 45-46.

[10] Li, L.; Kilbourn, R. G.; Adams, J.; and Fidler. I. J. "Role of Nitric Oxide in Lysis of Tumor Cells by Cytokine-activated Endothelial Cells", *Cancer Research*, **1991**, 52, 2531-2535.

[11] Struer, D. J.; and Nathan, C. F. "Nitric Oxide: a Macrophage Product Responsible for Cytostasis and Respiratory Inhibition in Tumor Target Cells", *J. Exp. Med*., **1989**, 169, 1543-1555.

[12] Feldman, P. L.; Griffith, O. W.; Stuehr, D. J. "The Surprising Life of Nitric Oxide", *Chem. & Eng. News*, **1993**, Dec. 20, 26-38.

[13] Kerwin, J. F.; Lancaster Jr., J. R.; and Feldman, P. L. "Nitric oxide: a new paradigm for second messenger", *J. Med. Chem.*, **1995**, 4343-4362

[14] Gaston, B.; Reilly, J.; Drazen, J. M.; Fackler. J.; Ramdev, P.; Arnelle, D.; Mullins, M.; Sugarbaker, D. J.; Chee, C.; Singel, D. J.; Loscazo, J.; and Stamler, J. S. "Endogeneous nitrogen oxides and bronchodilatoe S-nitrosothiols in human airways", *Proc. Natl. Acad. Sci. USA*, **1993**, 90, 10957-10961.

[15] Stamler, J. S.; Jaraki, O.; Osborne, J.; Simon, D. I.; Keaney, J.; Vita, J.; Singel, D.; Valeri, C.; R.; and Loscalzo, J. "Nitric Oxide Circulates in Mamalian Plasma Primarily as an S-nitroso Adduct of Serum Albumin", *Proc. Natl. Acad. Sci. USA.*, **1992**, 89, 7674-7677.

[16] McCoustra, M. R. S.; and Pfab. "Photodissociation of Methyl and t-Butyl Thionitrite Near 450 nm", *J. Chem. Phys. Letters*, **1987**, 137, 355-360

[17] A natural question is how a *photodynamic* process leading to NO release occurs in sunlight. In fact, skin capillaries, which serve to regulate body temperature and nurture what is arguably the body's biggest organ, are close enough to the surface such that exposure to daylight must cause significant events, as we now show. The chromophore is S-nitrosoalbumin, for which GSNO is a model. We calculated the photocleavage rate based on the following parameters: 100 micron penetration (1/e) of 350 nm light into the skin, and the 500 micron penetration (Bensasson, R.Vet al.., Excited States and Free Radicals in Biology and Medicine Oxford Science, 1993) of 550 nm light at sea level solar intensities of 30 and 300 W/(m^2 eV), respectively, see Linsebigler, A. Let al *Chem. Rev.*, **1995**, *95*, 735-758; we assume a 10% composition of blood in skin; and $\varepsilon_{350,\,SA\text{-}NO} = 4000\ M^{-1}\ cm^{-1}$ and $\varepsilon_{550,\,SA\text{-}NO} = 50\ M^{-1}\ cm^{-1}$ [SA-NO]=10^{-5} M and a quantum yield of NO/NO^+ escape from photoexcited Cys-NO of BSA-NO that is 0.09, see Stamler, J. S. et al *Proc. Natl. Acad. Sci. USA.*, **1992**, *89*, 7674-7677. We find that the rate of NO photocleavage from SA-NO equals that from the cysteine ← SA-NO transnitrosation pathway (~1 μM/hour) and exceeds that of the glutathione ← SA-NO pathway. The thermolytic rates may be found in Joshi, U. M. et al *Int. J. Biochem.*, **1987**, *19*, 1029-1035. *Thus, the photolytic process in skin can be competitive with other known transnitrosation pathways.*

[18] Cambel, S. S.; and Murphy, P. J. "Extraocular Circadian Phototransduction in Humans", *Science*, **1998**, 279, 396-399.

[19] Goldstein, S.; and Czapski, G. "Mechanism of the Nitrosation of Thiols and Amines by Oxygenated ·NO Solutions: the Nature of the Nitrosating Intermediates", *J. Am. Chem. Soc.*, **1996**, 118, 3419-3425.

[20] Stamler, J. S., Simon, D. I.; Osborne, J. A.; Mullins, M. E.; Jaraki, O. J.; Michel, T.; Singel, D.; and Localzo, J. "S-Nitrosylation of proteins with nitric oxide:Synthesis and characterization of biologically active compounds", *Proc. Natl. Acad. Sci. USA.*, **1992**, 89, 444-448.

[21] Park J-W.; Billman, G. E.; and Means, G. E. "Transnitrosation as a predominant mechanism in the hypotensive effect of S-nitrosoglutathione.", *Biochemistry and Molecular Biology International*, **1993**, 30(5), 885-891.

[22] Williams, D. L. H. "S-ni trosation and the reactions of S-Nitroso Com pounds", *Chem. Soc. Rev.*, **1985**, 14, 171-197.

[23] Morris, P. A.; and Williams, D. L. H. "", *J. Chem. Soc. Perkin Trans.*, **1988**, 2, 513.

[24] Larsson, A.; Orrenius, S.; Holm gren, A.; and Mannervik, B. Eds. Function of Glutathione. Biochemical, Hysiological, Toxicological and C linical Aspect (Raven Press, New York, 1983)

[25] Peters, T. Jr. All About Albumin (Academic Press, 1996)

[26] Carter, D.C.; He, X.; Munson, S. H.; Twigg, P. D.; Gernet, K. M.; Broom , M. B.; and Miller, T. "Three-Dim ensional Struc ture of Hum an Serum Albumin", *Science*, **1989**, 244, 1195-1198.

[27] Xiao, M. H.; and Ca rter, D. C. "Atom ic Structure and Che mistry of Hum an Serum Albumin", Nature, **1992**, 358, 209-215.

[28] Gosselet, M .; Mahieu, J. P.; and Sebille, B. "Reactiv ity of arom atic and hetero cyclic disulfide with thiol group of bovine serum albumin", *Int. J. Biol. Macromol.*, **1990**, 10, 241-247.

[29] Bonnett, R.; and Nicolaidou, P. "Nitrite and the Environment. The Nitrosation of a-am ino Acid Derivatives", *Heterocycles*, **1977**, 7(1), 637-659.

[30] Sexton, D. J.; Muruganandam , A.; McKenney, D. J.; and Mutus, B. "Photolysis of the films: Evidence for cyano radi cal, cyanide ion and nitric oxi de loss and redox pathw ays", *Photochem. and Photobiol.*, **1994,** *59*, 463-467.

[31] Rosenfeld, L. Z. *Physik* **1928,** 52, 161.

[32] Mohney, B. K.; and W alker, G. C. "Confor mational Restriction of Cysteine-Bound NO in Bovine Serum Album in Reveal ed by Circular Dichroism ", *J. Amer. Chem. Soc.***, 1997**, 119(39), 19311-9312.

[33] *Gaussian 94*, Revision D.4, M. J. Frisch, G. W . Trucks, H. B. Schlegel, P. M. W . Gill, B. G. Johnson, M. A. Robb, J. R. Cheesem an, T. Keith, G. A. Peterss on, J. A. Montgom ery, K. Raghavachari, M. A. Al-Laham , V. G. Zak rzewski, J. V. Ortiz, J. B. Fores man, J. Cioslowski, B. B. Stefanov, A. Nanayakkara, M. Challacombe, C. Y. Peng, P. Y. Ayala, W. Chen, M. W. Wong, J. L. Andres, E. S. Replog le, R. Gomperts, R. L. Martin, D. J. Fox, J. S. Binkley, D. J. De frees, J. Baker, J. P. Stewart, M. Head-Gordon, C. Gonzalez, and J. A. Pople, Gaussian, Inc., Pittsburgh PA, 1995.

[34] Schinke, R.; Henning, S.; and Untch, A. "Diffuse vibrational structures in photoabsorption spectra: A comparison of CH_3ONO and CH_3SNO using two-dimensional *ab initio* potential energy surfaces", *J. Chem. Phys.*, **1989**, 91(4), 2016-2029.

[35] Spartan 5.0.1, W avefunction, Inc.18401 Von Ka rman Ave., Ste. 370, Irvine, CA 92612 U.S.A

[36] Dalton: "An electronic structure program , Release 1.0 (1997)", written by T.Helgaker, H.J.Aa.Jensen, P.Jørgensen, J.Olsen, K.R uud, H.Ågren, T.Andersen, K.L.Bak, V.Bakken, O.Christiansen, P.Dahle, E.K.Dalskov, T.Enevoldsen, B.Fernandez, H.Heiberg, H.Hettema, D.Jonsson, S.Kirpekar, R.Kobayashi, H.Ko ch, K.V.Mikkelsen, P.Norm an, M.J.Packer, T.Saue, P.R.Taylor, and O.Vahtras

[37] Bak, K. L.; Hansen, Aa. E.; Rudd, K.; Helgaker, T.; Olsen, J.; and Jorgensen, P. J. "Ab initio calculation of electronic circular dichroism for trans- cyclooctene using London atomic orbitals", *Theor. Chim. Acta*., **1995**, 90, 441

[38] Akhremitchev, B.; Wang, C.; and Walker, G. C. "A Femtosecond Absorption Spectrometer Tunable from 50,000 – 800 cm^{-1}: Nonlinear Optics and Pump/Probe Geometries", *Rev. Sci. Inst.*, **1996**, *67*, 3799.

[39] Andrews, L.; Hassanzadeh, P.; Brabson, G. D.; Citra, A.; and Neurock, M. "Reactions of Nitric Oxide with Sulf ur Species Inf rared Spectr a And Density Functiona l Theory Calculations of SNO, SNO^+, and SNNO in Solid Argon", *J. Phys. Chem.*, **1996**, 100, 8273-8279.

[40] deOliveira, M. G.; Langley, G. J.; and Rest, A. J. "Photolysis of the [Fe(CN)5(NO)](2-) ion in water and poly(vinyl alcohol) films: Evidence for cyano radi cal, cyanide ion and nitric oxide loss and redox pathways", *J. Chem. Soc. Dal. Trans.*, **1995**, 2013-2019.

[41] Lim, M.; Jackson, T.; and Anfinrud, P. "Ultrafast rotation and trapping of carbon monoxide dissociated from myoglobin.", *Nature Structural Biology*, **1997**, 4(3), 209-214.

[42] Hydrogen bond life-times of 1.4 ps have been observed in simulation of aqueous sovation of CN^-. (Ferrario, M.; Klein, M. L.; McDonald, I. R. *Chem. Phys. Lett.*, **1993**, 213, 537).

[43] Hoffman, M. Z. and Hayon, E. "One-Electr on Reduction of the Di sulfide Linkage in Aqueous Solution. Form ation, protonation, and Decay Kinetics of the $RSSR^-$ Radical", *J. Phys. Chem.* **1973,** *77*, 990-996

[44] Anisotropy data are obtained by measuring the polarized probe absorbances parallel (||) and perpendicular ($\perp$) to th e polarized pu mp pulse and determ ining the m ean angle between the pum ped and probed transition di pole m oments using the relation $\langle \cos^2[\Theta(t)] \rangle = (1+5r(t))/3$, where $r(t) = (I_{\parallel} - I_{\perp})/(I_{\parallel} + 2I_{\perp})$.

[45] Wood, P. D.; Mutus, B.; and Redm ond, R. W. "The Mechanism of Phot ochemical Release of Nitric Oxide from S-Nitrosoglutathione", *Photochem. and Photobiol.*, **1996**, 64(3), 518-524.

[46] Zhang, Y. Y.; Xu, A. M.; Nom en, M.; W alsh, M.; and K eany, J. F. Jr. "Nitrosation of Tryptophan Residue(s) in Serum Al bumin and Model Dipeptides", *Journal of Biological Chemistry*, **1996**, 271, 14271-14272.

[47] Lewis, J. W.; Goldbeck, R. A.; and Kliger, D. S. "Tim e-resolved circular dichroism spectroscopy: experiment, theory, and a pplications to biological system s", *J. Phys. Chem.*, **1992**, 96, 5243-5254.

[48] Esquerra, R. M.; Lewis, J. W .; and Kliger, D. S. "An improved linear retarder for time-resolved circular dichroism studies", *Rev. Sci. Inst.*, **1997**, 68, 1372-1376.

[49] Wen, Y. X.; Chen, E.; and Lewis, J. W . "Nanosecond time-resolved circular dichroism measurements using an upconverted Ti:sapphire laser", *Rev. Sci. Inst.*, **1996**, 67, 3010-3016.

[50] Xie X.; and Simon, J. D. "Picosecond Circular Dichroism Spectroscopy: a Jones Matrix Analysis", *J. Opt. Soc. Am. B.*, **1990**, 7, 1673-1684.

[51] Xie, X.; and Simon, J. D. "Protein Conformational Rel;axation following Photodissociation of CO from Carbonmonoxymyoglobin: Picosecond Circular Dichroism and Absorption Studies", *Biochem.*, **1991**, 30, 3682-3692.

[52] Xie, X.; and Simon, J. D. "A picosecond circular dichroism study of photosynthetic rection centers from *Rhodobacter sphaeroides*", *Biochemica et Biophysica Acta*, **1991**, 1057, 131-139.

APPENDIX A

Detailed corrdinates of cysteine-NO used in various calculation

The detailed coordinates of the cis and trans conformer used in m ost calculation is as follow:

		TRANS Conformer			**CIS Conformer**		
Atom Number	**Atomic Number**	**X**	**Y**	**Z**	**X**	**Y**	**Z**
1	7	-0.8225	1.74079	-0.4525	-0.4938	1.7048	-0.3781
2	6	-1.0582	0.70678	0.52733	-0.8204	0.65966	0.56146
3	6	-2.0008	-0.3385	-0.0522	-1.9469	-0.2111	0.02018
4	8	-1.7161	-1.4846	-0.1989	-1.9095	-1.4001	-0.0159
5	1	-0.2366	1.4224	-1.1979	-0.0925	1.34161	-1.2192
6	8	-3.1882	0.15069	-0.3552	-2.9984	0.48357	-0.3701
7	1	-0.4016	2.54669	-0.0387	0.14823	2.35891	0.01942
8	1	-1.5993	1.16294	1.35184	-1.2369	1.14172	1.44351
9	6	0.18438	0.03123	1.12307	0.34331	-0.217	1.04382
10	16	1.28595	-0.744	-0.0919	1.25873	-1.0572	-0.2759
11	7	2.63477	0.35311	0.12869	2.67572	-0.0681	-0.5011
12	1	0.78493	0.77302	1.63617	1.05588	0.39222	1.58358
13	1	-0.1054	-0.7256	1.83859	-0.0129	-0.9953	1.70373
14	1	-3.7185	-0.5474	-0.7166	-3.66	-0.1233	-0.6755
15	8	3.56208	0.11118	-0.5366	2.77399	0.91066	0.13113